The Choline-binding Protein PspC of Streptococcus pneumoniae Interacts with the C-terminal Heparin-binding Domain of Vitronectin

Voss, Sylvia; Hallstroem, Teresia; Saleh, Malek; Burchhardt, Gerhard; Pribyl, Thomas; Singh, Birendra; Riesbeck, Kristian; Zipfel, Peter F.; Hammerschmidt, Sven

Published in:
Journal of Biological Chemistry

DOI:
10.1074/jbc.M112.443507

2013

The choline-binding protein PspC of *Streptococcus pneumoniae* interacts with the C-terminal heparin-binding domain of vitronectin*

Sylvia Voß[1], Teresia Hallström[2], Malek Saleh[1], Gerhard Burchhardt[1], Thomas Pribyl[1], Birendra Singh[4], Kristian Riesbeck[4], Peter F. Zipfel[2,3], and Sven Hammerschmidt[1$]

From the [1]Department Genetics of Microorganisms, Interfaculty Institute for Genetics and Functional Genomics, University of Greifswald, D-17487 Greifswald, Germany, [2]Department of Infection Biology, Hans Knoell Institute, Leibniz Institute for Natural Product Research and Infection Biology, D-07745, Jena and [3]Institute for Microbiology, Friedrich Schiller University, D-07743 Jena, Germany, [4]Medical Microbiology, Department of Laboratory Medicine Malmö, Lund University, Skåne University Hospital, SE-205 02 Malmö, Sweden

Running title: Pneumococcal PspC binds vitronectin

[$]To whom correspondence should be addressed: Prof. Dr. Sven Hammerschmidt, Department Genetics of Microorganisms, Interfaculty Institute for Genetics and Functional Genomics, Ernst Moritz Arndt University Greifswald, Friedrich-Ludwig-Jahn-Strasse 15A, 17487 Greifswald, Germany, Phone: 0049-3834-864161, Fax: 0049-3834-864172, E-mail: sven.hammerschmidt@uni-greifswald.de.

Keywords: *Streptococcus pneumoniae*, pneumococcal surface protein C, PspC, adhesion, vitronectin complement

Background: Adhesins are essential for pneumococcal colonization and pathogenesis.
Results: PspC, identified as vitronectin-binding protein, interacts with the C-terminal heparin-binding domain of vitronectin, and, when bound to PspC, it retains complement inhibitory function.
Conclusion: PspC is an adhesin for vitronectin and the PspC-vitronectin interaction inhibits immune attack.
Significance: The PspC-vitronectin interaction provides new insights into pneumococcal adhesion and complement inhibition.

SUMMARY

Adherence of *Streptococcus pneumoniae* is directly mediated by interactions of adhesins with eukaryotic cellular receptors or indirectly by exploiting matrix and serum proteins as molecular bridges. Pneumococci engage vitronectin, the human adhesive glycoprotein and complement inhibitor, to facilitate attachment to epithelial cells of the mucosal cavity, thereby modulating host cell signaling. In this study, we identified PspC as vitronectin-binding protein interacting with the C-terminal heparin-binding domain of vitronectin. PspC is a multifunctional surface-exposed choline-binding protein displaying various adhesive properties. Vitronectin-binding required the R domains in the mature PspC protein, which are also essential for the interaction with the ectodomain of the polymeric immunoglobulin receptor and secretory IgA. Consequently, secretory IgA competitively inhibited binding of vitronectin to purified PspC and to PspC-expressing pneumococci. In contrast, Factor H, that binds to the N-terminal part of mature PspC molecules, did not interfere with the PspC-vitronectin interaction. Using a series of vitronectin peptides, the C-terminal heparin-binding domain was shown to be essential for the interaction of soluble vitronectin with PspC. Binding experiments with immobilized vitronectin suggested a region N-terminally to the identified HBD as additional binding region for PspC, suggesting that soluble, immobilized as well as cellularly bound vitronectin possess different conformations. Finally, vitronectin bound to PspC was functionally active and inhibited the deposition of the terminal complement complex. In conclusion, this study identifies and characterizes (on the molecular level) the interaction between the pneumococcal adhesin PspC and the human glycoprotein vitronectin.

Streptococcus pneumoniae (*S. pneumoniae*, pneumococci) are Gram-positive bacteria usually transmitted by aerosols and

asymptomatically colonizing the human upper respiratory tract. Especially in children, the elderly and immunocompromised adults pneumococci can cause mild local infections such as sinusitis or otitis media but also severe life-threatening diseases including community-acquired pneumonia (CAP), pneumococcal meningitis, and sepsis (1). After surmounting the airway mucus and initial loose attachment to the host cell surface, nasopharyngeal colonization by *S. pneumoniae* proceeds by an intimate contact to the respiratory epithelium. Therefore, pneumococci express an armamentarium of surface-exposed adhesins. These adhesins interact with host cellular receptors directly or indirectly by targeting extracellular matrix or acquiring human serum proteins, thereby linking pneumococci to eukaryotic cell receptors or professional phagocytes (2-8). Adhesive properties are known for a number of pneumococcal surface proteins recognizing plasmin(ogen), fibronectin, thrombospondin-1, and vitronectin (8-17). A subpopulation of pneumococci produces pili, encoded by pilus islet (PI)-1 or PI-2, and at least the RrgA of PI-1 functions as an adhesin (17-20). However, one of the most important adhesins of *S. pneumoniae* is the pneumococcal surface protein C (PspC, also referred to as CbpA or SpsA), which belongs to the family of pneumococcal choline-binding proteins (CBPs). Eleven different PspC subtypes are classified into two subgroups, dependent on their anchorage to the bacterial cell envelope. The classical PspC proteins (subtypes 1-6, members of subgroup I) contain a conserved C-terminal choline-binding domain (CBD) with a variable number of 7-13 repeats, each of 20 amino acid residues. The CBD enables a non-covalent attachment to phosphorylcholine moieties on the bacterial surface. In contrast, PspC-like proteins (subtypes 7-11, members of subgroup II) possess the C-terminal sortase recognition motif LPXTG, and are therefore covalently linked to the bacterial peptidoglycan via the sortase-catalyzed transpeptidation reaction. PspC proteins of subgroup I share high similarities in sequence, structure and organization of the N-terminal region: the 37-aa leader peptide is followed by the Factor H-binding domain, one or two single repeated domains (termed R1 and R2) and a proline-rich region (21, 22). Pneumococcal adhesion and internalization into respiratory epithelial cells is primarily accomplished by the unique, human specific binding of PspC to the secretory component (SC) of the polymeric Ig receptor (pIgR) (23, 24). A conserved hexapeptide motif contained once in each R domain within PspC directly interacts with the human Ig-like domains D3 and D4 of the SC (either soluble or bound to the pIgR or as part of the mucosal secretory IgA) (24-26). The PspC-pIgR interaction mediates adherence and activation of signal transduction cascades resulting in the uptake and transcytosis of pneumococci across the epithelial barrier (2, 25, 26). Further, PspC interacts directly with a laminin-specific integrin-receptor ubiquitously expressed on vascular endothelial cells, contributing to invasive diseases, including pneumococcal meningitis (27). In addition, PspC recruits the complement inhibitor proteins C4b-binding protein (C4BP) and Factor H to the bacterial surface (28, 29). The interaction sites were mapped to a 121-aa sequence in the N-terminal part of the PspC protein and to the short consensus repeats (SCRs) 8-11 and SCRs 19-20 of Factor H (2, 30). This interplay enables pneumococci to effectively evade the host immune attack and to control complement effector functions by inhibiting the C3 convertase activity of the alternative pathway (31). Moreover, Factor H bound to the pneumococcal surface facilitates adherence to human integrins of epithelial cells (2, 30).

Pneumococci are able to recruit soluble vitronectin (Vn) to their surface. However, only host-cell bound vitronectin facilitates pneumococcal adherence to and invasion into respiratory epithelial cells. Vitronectin circulates in human plasma as a folded monomer of 75 kDa, existing either as a single-chain protein or as a two-chain disulfide-linked polypeptide (65+10 kDa), and modulates the complement, fibrinolytic and coagulation system (32, 33). On the other hand, in its multimeric, unfolded form, vitronectin can efficiently bind to and incorporate into the extracellular matrix (ECM) of various human tissues supporting cell adhesion and differentiation, as well as regulating ECM composition and stability (32, 33). The interaction sites for a vast variety of binding partners are located in different vitronectin domains. The N-terminal part comprises a somatomedin B domain and an RGD-motif that allows attachment of vitronectin to the integrin receptors $\alpha_v\beta_3$, $\alpha_v\beta_1$, and $\alpha_v\beta_5$ (34). In addition to four hemopexin-

type repeats, vitronectin consists of three heparin-binding domains (HBDs), of which the most C-terminal one mediates binding to proteoglycans and is involved in ligand-induced multimerization of the molecule (33, 35). Gram-negative pathogenic bacteria recruit plasma vitronectin to prevent the assembly and deposition of the terminal complement complex (TCC) and subsequent bacterial lysis. Recently, *Haemophilus influenzae* Protein E (PE) was identified as a vitronectin-binding protein, and it was demonstrated that PE exclusively interacts with the C-terminal heparin-binding domain of vitronectin (36-38). Gram-positive pathogens commonly utilize ECM-associated vitronectin for an efficient adhesion to host epithelial cells and subsequent internalization (39). Binding of *S. pneumoniae* to host-cell-bound vitronectin particularly engages the $\alpha_v\beta_3$-integrin receptor triggering the activation of the integrin-linked kinase (ILK) in a PI3-kinase-dependent manner. In addition, upon infection of host cells, pneumococci induce protein kinase B (Akt) activation, resulting in a rearrangement of the cellular actin cytoskeleton and formation of microspike-like membrane protrusions in which pneumococci are subsequently trapped. The pneumococcal binding site in vitronectin was restricted to the heparin-binding domain(s) of vitronectin (4). However, as mentioned above, the pneumococcal surface factor that binds human vitronectin has not yet been described.

In this study, we identified the multifunctional PspC of *S. pneumoniae* as a human vitronectin-binding protein. In addition, we demonstrated that vitronectin preferentially binds to PspC subtypes of *S. pneumoniae* consisting of two SC-binding regions, termed R domains, located in the mature N-terminal part of PspC. We localized the major binding site of PspC to the C-terminal heparin-binding domain of vitronectin. The data further suggested that a region N-terminally to the C-terminal HBD confers binding of pneumococci via PspC to immobilized vitronectin. Finally, we confirmed that vitronectin bound to PspC is functionally active and can inhibit the terminal complement pathway.

EXPERIMENTAL PROCEDURES

Bacterial strains, culture conditions and pneumococcal mutant construction— *S. pneumoniae* were cultured on solid blood agar plates (Oxoid, Germany) at 37°C and 5% CO_2 or in liquid Todd-Hewitt-broth (Roth, Germany) supplemented with 0.5% yeast extract (Roth) to mid-log phase (3.5-4 x 10^8 cfu/ml). Pneumococcal wild-type strains, isogenic mutants deficient for the capsular polysaccharide (Cps), PspC, functional lipoproteins, or LPxTG-anchored proteins, respectively, are listed in Table 1. Primers used to amplify DNA fragments are listed in Table 2. Pneumococcal mutants in R800 and D39Δ*cps* were generated by insertion deletion mutagenesis of the respective genes. For the construction of R800Δ*pspC*, the pQSV22 plasmid was constructed by ligation of the *Spe*I-linearized and blunt-ended *pspC* gene, which was formerly cloned into pQE-30 (23), with the *Eco*RV digested spectinomycin resistance gene *aad9* (Table 1). To construct the mutant D39Δ*cps*Δ*lgt*, a 1940-bp fragment containing the *lgt* gene region interrupted by an *ermB* gene cassette was PCR-amplified from genomic DNA of *S. pneumoniae* R6Δ*lgt* with the primers lgt1fw and lgt7rev and cloned into the TA-cloning vector pGEM-T easy resulting in plasmid p552 (Table 1). For the construction of D39Δ*cps*Δ*lsp*, the *lsp* gene region was amplified from D39Δ*cps* genomic DNA using the primers lsp1fw and lsp4rev and cloned into pGEM-T easy. By inverse PCR, an internal part of the *lsp* gene was deleted using the primer pair lsp2rev and lsp3fw with incorporated *Cla*I restriction sites for subsequent ligation with the *aad9* gene, amplified with the primers SpcforClaI and SpcrevClaI, with the PCR product. This resulted in plasmid p556 (Table 1). To construct a mutant deficient for surface-expression of LPxTG-anchored proteins in D39Δ*cps*, the *srtA* gene region (1350 bp) was amplified from TIGR4 genomic DNA using the primers SP_1218StartFor and SP_1218EndRev. After cloning the PCR product into pBlue-Script II TKS(-), the primers SP_1218StartRev and SP_1218EndFor, which incorporated *Asc*I restriction sites, were used to replace an internal sequence in *srtA* with an *ermB* gene cassette amplified with the primer pair EryfwdAscI and EryrevAscI. This resulted in plasmid p745 (Table 1).

S. pneumoniae strains were transformed either with the plasmid constructs or linear DNA fragments amplified by PCR in the presence of competence-stimulating peptide-1

as described previously (40). Gene knockouts of pneumococcal transformants were verified by PCR and, where applicable, by flow cytometric analysis.

Escherichia coli strains, listed in Table 1, were cultivated at 30°C on Luria-Bertani agar or broth (Roth) supplemented with appropriate antibiotics. Transformation of *E. coli* strains with plasmid DNA was carried out with $CaCl_2$-treated competent cells according to standard procedures.

Culture conditions, cloning and recombinant procedures in Lactococcus lactis*—L. lactis* MG1363 was grown statically at 30°C in M17 agar or broth (Oxoid) supplemented with 0.5% glucose and 5 µg/ml erythromycin. Transformation with plasmid DNA was performed by electroporation as described recently (41). The recombinant pGKK1 plasmid was used for the inducible extracellular expression of PspC in *L. lactis* (41). To generate heterologous *L. lactis* expressing other PspC subtypes, the desired *pspC* DNA fragments were amplified by PCR using chromosomal DNA of strain *S. pneumoniae* ATCC33400 (PspC2) or D39 (PspC3). DNA was amplified with the primers N-PspC and PspCrev containing incorporated *Bam*HI and *Nco*I restriction sites, respectively. The PCR products were digested with *Bam*HI and *Nco*I (NEB) and cloned into the similarly digested pGKK1 vector to generate the pPspC2 or pPspC3 plasmid, respectively. The coding sequence of *psp*C was verified by DNA sequencing (Eurofins MWG Operon, Germany). Sequence comparisons were performed with the blast programs from the NCBI database. The recombinant plasmid was first selected after transformation into *E. coli* DH5α and then transformed into electrocompetent *L. lactis* (Table 1). Expression of PspC was induced by adding Nisin (0.1 µg/ml) to mid-log grown recombinant lactococci.

Reagents and antibodies—DNA and protein markers were from Fermentas (Thermo Fisher Scientific Inc., Leicestershire, UK). Coomassie brilliant blue R250 and bovine serum albumin (BSA) were purchased from Roth. Heparin (potassium salt) and HRP-conjugated rabbit anti-IgA antibodies were obtained from ICN Biomedicals (Aurora, OH, USA). Multimeric vitronectin was purchased from Millipore (Merck Millipore KGaA, Germany). Biotin-labeled multimeric vitronectin was provided by Loxo (Germany). Recombinant C-terminally His_6-tagged multimeric vitronectin fragments were heterologously expressed in HEK293T cells and purified as described (38). FITC (fluorescein isothiocyanate), choline chloride, human secretory IgA, paraformaldehyde (PFA), Nisin, heparan sulfate, chondroitin sulfate A, and Bradford Reagent were purchased from Sigma-Aldrich (Germany). Human Factor H was provided by Calbiochem (Merck Millipore KGaA, Germany) or Complement Technology (Tyler, TX, USA). Rabbit anti-human vitronectin antibodies were purchased from Abcam (Cambridge, UK) or Complement Technology. Goat anti-human Factor H antibodies and the complement inhibitor proteins C5b-6, C7, C8, and C9 were provided by Complement Technology. AlexaFluor488-conjugated goat anti-rabbit IgG was provided by Molecular Probes (Life Technologies, NY, USA). HRP-conjugated swine anti-rabbit antibodies, HRP-conjugated rabbit anti-goat antibodies, mouse anti-human C5b-9 monoclonal antibodies, and HRP-conjugated swine anti-mouse antibodies were purchased from Dakopatts (Glostrup, Denmark). Cy5-conjugated goat anti-mouse antibodies and AlexaFluor488-conjugated streptavidin were provided by Dianova (Germany). The ELISA substrate 1,2-phenylenediamine dihydrochloride (OPD) was purchased from DakoCytomation (Glostrup, Denmark). Anti-SH2 and anti-SH12 antiserum were generated by immunization of mice with PspC-SH2 or -SH12 protein derivative according to standard methods. Mouse control serum was generated by similar immunization procedure without protein.

Expression of N-terminally His_6-tagged proteins and protein purification—N-terminally His_6-tagged PspC proteins used in this study have been described earlier (Fig. 3A) (24, 25). Briefly, the recombinant His_6-tagged PspC proteins represent PspC group 2, which is expressed by strain ATCC 33400 (serotype 1), or PspC group 3 expressed by strain NCTC 10319 (serotype 35A) and D39 (serotype 2), respectively. The His_6-tagged fusion proteins were purified by Ni^{2+} affinity chromatography either with the Protino Ni prepacked column kit according to the manufacturer's instructions (Macherey-Nagel) or with His Trap FF crude columns (GE Healthcare) and Äktapurifier (GE Healthcare). Proteins were dialyzed against appropriate buffers before experiments and concentrations were measured by UV absorbance (280 nm)

using a Nano-drop spectrophotometer (Thermo Scientific, Wilmington, DE, USA). The concentrations were also verified using a Bradford protein assay. The purity of expressed proteins was controlled on SDS-PAGE stained with Coomassie brilliant blue R250 or silver nitrate.

Flow cytometric analysis—To detect vitronectin bound to pneumococci, 1 x 10^8 bacteria were incubated with vitronectin or recombinant vitronectin peptides, respectively, in 100 µl Dulbecco's modified Eagle medium (DMEM, 1 g/l glucose; PAA Laboratories) for 45 min at 37°C in 96-well plates (Greiner, Germany), washed, and incubated with anti-human vitronectin antibodies. After washing, bacteria were incubated with AlexaFluor488-conjugated anti-rabbit IgG. To inhibit vitronectin-binding, pneumococci were incubated with vitronectin (2.5 µg/ml) in DMEM supplemented with 5% choline chloride (ChoCl). In further inhibition experiments, pneumococci were incubated with secretory IgA (sIgA), anti-PspC mouse antiserum or mouse control serum (both at a dilution of 1:50) for 15 min prior to addition of vitronectin (1 µg/ml), or vitronectin (1 µg/ml) was incubated for 15 min in presence of purified His_6-tagged PspC-SH13, and added to the pneumococci. After washing, bacteria were incubated with anti-human vitronectin antibodies, and afterwards incubated with AlexaFluor488-conjugated anti-rabbit IgG. In inhibition experiments with Factor H, pneumococci were incubated for 15 min with Factor H, thereafter biotin-labeled vitronectin (1 µg/ml) was added to the pneumococci. After extensive washing, bacteria were incubated with AlexaFluor488-conjugated streptavidin (2 µg/ml). Finally, bacteria were washed and fixed using 1% PFA overnight at 4°C. The samples were analyzed by flow cytometry using a FACS Calibur™ (Becton Dickinson). Data acquisition was conducted using the CellQuestPro Software 6.0 (Becton Dickinson) and data analysis was performed using the WinMDI Software 2.9 (The Scripps Research Institute). The bacteria were detected and gated as described previously (4, 15) and the results of protein binding to pneumococci are shown as the total fluorescence (geometric mean fluorescence intensity (GMFI) multiplied with the percentage of AlexaFluor488-labeled and gated events) or as percentage vitronectin-binding.

Enzyme-linked immunosorbent assay (ELISA)—Microtiter plates (F96, Polysorb™, Nunc-Immuno Module) were coated with 100 µl of 5 µg/ml *S. pneumoniae* PspC constructs PspC-SH2, SH3, SM1, SM2, SH12, SH13, *H. influenzae* PE, or *Staphylococcus aureus* binder of IgG (Sbi), respectively, over night at 4°C. The plates were washed four times with 0.05% Tween® 20/PBS (pH 7.4) and blocked for 1 h at room temperature (RT) with 0.1% Tween® 20/PBS supplemented with 2% BSA (blocking buffer). After washings, the plates were incubated for 1 h at RT with vitronectin (100 µl of 0-40 µg/ml) or the various recombinant vitronectin constructs (100 µl of 5 µg/ml) diluted in blocking buffer. Thereafter, the wells were washed and incubated with a rabbit anti-human vitronectin antibodies (1:1000 in blocking buffer) followed by HRP-conjugated anti-rabbit antibodies (1:1000 in blocking buffer). The reaction was developed with OPD and the absorbance was measured at 492 nm. In inhibition assays, immobilized SH13 was incubated with increasing concentrations of NaCl (100 µl of 0-1.0 M), heparin (100 µl of 0-5000 µg/ml), heparan sulfate or chondroitin sulfate A (both 100 µl of 0-1000 µg/ml) and a constant concentration of vitronectin (5 µg/ml). Since Factor H does not bind to the recombinant PspC-SH13 fragment in ELISA, the Factor H-binding derivative PspC-SH12 (30) was used for the competition assays to elucidate the effect of Factor H and sIgA on vitronectin-binding to immobilized PspC. Vitronectin, used at different concentrations (100 µl of 0-40 µg/ml), was incubated with a constant amount of Factor H (10 µg/ml) or sIgA (5 µg/ml) and binding to immobilized PspC-SH12 was measured using goat anti-human Factor H antibodies (1:2000) and HRP-conjugated anti-goat antibodies (1:2500) followed by development with OPD. Bound sIgA was detected with HRP-conjugated anti-IgA antibodies (1:1000). The reaction was developed with OPD.

Surface plasmon resonance—The direct protein–protein interactions between vitronectin or vitronectin fragments and His_6-tagged PspC protein derivatives were analyzed by SPR using a Biacore T100 optical biosensor. Covalent immobilization of proteins on a carboxymethyl dextran (CM5) sensor chip was performed by a standard amine-coupling procedure as described previously (4). Briefly, vitronectin (5 µg/ml), Vn^{80-396}, Vn^{80-339} or Vn^{80-229} (each 25 µg/ml), PspC-SH13

(30 µg/ml) or PspC-SM2 (50 µg/ml) were coupled in 10 mM sodium acetate, pH 4.0, onto a N-hydroxysuccinimide (NHS, 0.05 M)/N-ethyl-N′(diethylaminopropyl)carbodiimide (EDC, 0.2 M)–activated CM5 sensor chip at a flow rate of 10 µl/min. The control flow cell was prepared in the same way but without injecting the protein. Binding of the analytes was performed in 0.05% Tween® 20/PBS (pH 7.4) or HNET buffer (50 mM HEPES, 150 mM NaCl, 3 mM EDTA, 0.005% Tween®20, pH 7.5) at 25°C using a flow rate of 10 µl/min or 30 µl/min. The affinity surface was regenerated between subsequent sample injections of proteins with 12.5 mM sodium hydroxide or 2 M NaCl. Each interaction was measured at least three times. The sensorgrams show the response unit (RU) values after subtraction of the blank run and value(s) without protein(s) from the corresponding sensorgrams. Binding was analyzed using the BiacoreT100 Evaluation Software (Version 2.0.1.1).

Binding of bacteria to immobilized human proteins—Microtiter plates (F96, MaxiSorp™, Nunc-Immuno Module) were coated with 100 µl of 10 µg/ml human vitronectin or recombinant vitronectin peptides in 0.1 M sodium carbonate-bicarbonate buffer (pH 9.2) at 4°C overnight. The surfaces of the wells were subsequently blocked with 1% BSA/PBS (pH 7.4) for at least 3 h at room temperature. Labeling of the bacteria with FITC was performed as described previously (15). Extensively washed FITC-labeled bacteria (100 µl of 2 x 10^8 bacteria) were added to the washed wells and incubated for 1 h at 37°C for binding. Fluorescence was measured at 485 nm/520 nm (excitation/emission) using a multidetection microplate reader (Fluostar Omega, BMG Labtech, Germany). Measurements were done prior to the first washing step (total fluorescence of inoculum) and after each of the four washing steps with 100 µl PBS (fluorescence of bound bacteria).

TCC deposition assay—Microtiter plates (F96, Medisorb™, Nunc-Immuno Module) were coated with PspC-SH12 (100 µl of 5 µg/ml) over night at 4°C. The plates were washed four times with 0.05% Tween® 20/PBS and blocked for 1 h at RT with 2% BSA/0.05% Tween® 20/PBS. After washings, the plates were incubated for 1 h at RT with vitronectin (100 µl of 0-50 µg/ml) or Factor H (100 µl of 0-50 µg/ml). Thereafter, the wells were washed and incubated with C5b-6 (1.5 µg/ml) and C7 (1 µg/ml) for 10 min at RT and thereafter C8 (0.2 µg/ml) and C9 (1 µg/ml) were added to a total volume of 100 µl and incubated for 30 min at 37°C. TCC deposition was detected with mouse anti-human C5b-9 mAb (1:1000) and HRP-conjugated swine anti-mouse antibodies (1:2500). The reaction was developed with OPD and the absorbance was measured at 492 nm.

Statistical analysis—All data are reported as mean ± SD. Results were statistically analyzed using the unpaired two-tailed Student's test. A P-value ≤ 0.05 was considered statistically significant.

RESULTS

Vitronectin binds to intact pneumococci—*S. pneumoniae* were previously shown to recruit multimeric vitronectin (4). These results were confirmed by flow cytometric analysis, which revealed a dose-dependent binding of vitronectin to the pneumococcal surface (Fig. 1*A;* supplemental Fig. S1*A*). To identify pneumococcal surface protein(s) interacting with soluble human vitronectin, pneumococci either lacking sortase-anchored surface proteins due to knockout of the sortase-encoding gene *srtA* or pneumococci deficient in surface-expression of functional lipoproteins were examined for vitronectin-binding using a flow cytometry-based binding assay. The nonencapsulated pneumococcal strain D39Δ*cps* and its isogenic mutants D39Δ*cps*Δ*lgt*, D39Δ*cps*Δ*lsp*, or D39Δ*cps*Δ*srtA* showed no differences in their ability to bind soluble vitronectin (Fig. 1*B*, supplemental Fig. S1*B*). In contrast, pretreatment of pneumococci with choline chloride (ChoCl), which removes non-covalently bound choline-binding proteins from surface-exposed, phosphorylcholine-decorated teichoic acids (supplemental Fig. S1*C*), resulted in significantly decreased vitronectin-binding (Fig. 1, *C* and *D*). Thus, these data suggest that CBPs contribute to vitronectin-binding to the pneumococcal surface.

PspC is a highly abundant, multifunctional CBP that mediates pneumococcal adhesion to and invasion into host cells but also immune evasion from the host complement. Remarkably, various pneumococcal strains deficient for PspC showed a significant lower vitronectin-binding activity compared to their isogenic wild-type strains as assessed by flow cytometry (Fig. 1*E*, supplemental Fig. S1*D*).

Similarly, pretreatment of wild-type strains expressing different PspC subtypes with mouse anti-PspC serum significantly decreased vitronectin-binding to the pneumococcal cell surface, whereas the control serum showed no effect (Fig. 1*F*, supplemental Fig. S1*E-H*). These results suggest that PspC is a pneumococcal vitronectin-binding protein.

Analysis of the PspC-vitronectin interaction—S. pneumoniae D39Δ*cps*, expressing the PspC3 subtype, bound efficiently vitronectin. Therefore, the recombinant PspC3 derivative SH13 (PspC-SH13) was used to investigate the PspC-vitronectin interaction. To competitively inhibit binding of vitronectin to pneumococci, D39Δ*cps* was incubated with vitronectin in the presence of increasing concentrations of PspC-SH13. Flow cytometric analysis indicated that PspC-SH13 inhibited binding of vitronectin to the pneumococcal cell surface. PspC-SH13 used at 0.8 μM inhibited vitronectin-binding to viable pneumococci by 40% (Fig. 2*A*, supplemental Fig. S2*A*). In addition, in an ELISA approach, a dose-dependent binding of vitronectin to immobilized PspC-SH13 was demonstrated. PE, recently identified as a vitronectin-binding adhesin of nontypeable *H. influenzae* (36, 37), also bound to vitronectin, whereas Sbi, a Factor H and C3 binding protein of *S. aureus* (42), did not interact with vitronectin (Fig. 2*B*). In a complementary approach, PspC-binding to immobilized vitronectin was analyzed by surface plasmon resonance (SPR) studies. Binding of PspC-SH13 to immobilized vitronectin was dose-dependent and suggests a high binding intensity between adhesin and vitronectin as illustrated by slow dissociation rates of PspC-SH13 (Fig. 2*C*).

Vitronectin preferentially interacts with PspC derivatives comprising two R domains—To analyze the PspC-vitronectin interaction in more detail and to localize the vitronectin-binding domain in PspC, various PspC subtypes and derivatives were produced as His_6-tagged proteins in *E. coli* and employed in binding experiments (Fig. 3*A*). The ELISA approach showed a dose-dependent vitronectin-binding to the immobilized PspC3 derivative SH13, while lower binding activities were measured for PspC derivatives containing only one or no R domain (Fig. 3*C*). SPR analysis was used to verify and compare the binding of the PspC derivatives PspC-SH13, SH2, SH3, and SM2 to immobilized vitronectin. The PspC-SH13 protein comprising the two R domains R1 and R2 showed a high binding activity to vitronectin as indicated by the prominent and fast association and the slow dissociation of the complex upon removal of the analyte. In contrast, PspC derivatives consisting of only one R domain (PspC-SH2, or SM2) or only the N-terminal part of the mature PspC protein (PspC-SH3) bound with lower intensity to immobilized vitronectin as compared to PspC-SH13 (Fig. 3*D*, supplemental Fig. S2*B-C*). Importantly, at a rather low micromolar concentration, PspC-SH13 (0.09 μM) showed a remarkably strong binding, whereas the other His_6-tagged PspC proteins, even used at higher molar concentrations, interacted with remarkably lower intensities with immobilized vitronectin (Fig. 3*D*, supplemental Fig. S2*B-C*).

PspC expressed on the surface of the heterologous expression system *Lactococcus lactis* retains its biological activities (41). To assess the differences of PspC subtypes and the role of the number of R domains on binding of vitronectin, PspC2 and PspC3, respectively, were fused to the LPSTG cell wall-anchoring motif of PspC11.4, also known as Hic, and expressed on the surface of *L. lactis* (Fig. 3*B*) (43). Binding of the various FITC-labeled recombinant *L. lactis* strains to immobilized vitronectin was examined. Lactococci expressing PspC showed a significantly increased binding to immobilized vitronectin as compared to the *L. lactis* control strain. However, this binding also revealed a significant difference between the two PspC subtypes. Lactococci expressing PspC3 on their surface bound significantly stronger to vitronectin than their PspC2-expressing counterparts (Fig. 3*E*). These data suggest that the R domains of PspC, which contain the SC-binding motif, are critical for the PspC-vitronectin interaction.

Vitronectin interacts with the SC-binding region in PspC3—In order to assess the important role of the R domains of PspC3 for the interaction with vitronectin, the effect of the two other PspC ligands Factor H and secretory IgA (sIgA) on vitronectin-binding to viable pneumococci was assayed by flow cytometry. In this approach, Factor H, which binds to a region N-terminal to the R domain(s) in the PspC protein, did not inhibit binding of biotin-labeled vitronectin to pneumococci (Fig. 4*A*, supplemental Fig.

S3*A*). In contrast, sIgA, which binds to a conserved hexapeptide motif within the R domain, dose-dependently reduced the recruitment of vitronectin to the bacterial surface. SIgA used at a concentration of 125 µg/ml inhibited vitronectin-binding to pneumococci by ~50% (Fig. 4*B*, supplemental Fig. S3*B*). To analyze whether Factor H and vitronectin bind concurrently to PspC, binding of vitronectin to immobilized PspC-SH12 in the presence of Factor H was investigated. Factor H did not inhibit the dose-dependent binding of vitronectin to the immobilized PspC3 derivative SH12 (Fig. 4*C*). In addition, Factor H bound dose-dependently to PspC-SH12 in the presence of vitronectin (data not shown). In contrast, binding of sIgA to immobilized PspC-SH12 was significantly reduced upon addition of increasing concentrations of vitronectin (Fig. 4*D*). Similarly, binding of vitronectin was diminished at increasing concentrations of sIgA and a constant amount of vitronectin (data not shown). These results demonstrate that sIgA, but not Factor H, competes with vitronectin for binding to PspC, thus suggesting that the R domain(s) of PspC are important for the interaction of pneumococci with human vitronectin.

The C-terminal heparin-binding domain of vitronectin is essential for the interaction with PspC3—To characterize the biochemical features of the PspC interaction with vitronectin, binding of vitronectin to immobilized PspC-SH13 was analyzed in presence of NaCl. Binding of vitronectin to PspC-SH13 was salt sensitive. Sodium chloride at 250 mM decreased vitronectin-binding by 20%, and in the presence of 1 M NaCl the interaction was inhibited by ~70% (Fig. 5*A*). Heparin inhibits the vitronectin-mediated adherence of pneumococci to epithelial cells (4). To examine whether heparin-binding site(s) of vitronectin are relevant for the interaction with PspC, the effect of heparin, heparan sulfate and chondroitin sulfate A, respectively, on vitronectin-binding to immobilized PspC-SH13 was tested. Indeed, all three glucosaminoglycans inhibited the binding of vitronectin to PspC (Fig. 5*B-D*) in a dose-dependent manner. Heparin at a concentration of 1 µg/ml reduced vitronectin-binding to immobilized PspC-SH13 by 80% (Fig. 5*B*). Vitronectin contains three heparin-binding domains named HBD 1, 2, and 3, and various bacteria recognize at least one of them to evade the host´s immune system or to indirectly link themselves to integrins for colonization and internalization (39). To localize which of the three HBDs in vitronectin is relevant for contacting PspC and to narrow down its binding motif, a series of recombinant fragments spanning the amino acid residues 80-396 of the vitronectin molecule (Fig. 5*E*) was examined for binding to immobilized PspC-SH13. The truncated vitronectin fragments Vn^{80-396}, Vn^{80-379}, Vn^{80-373}, and Vn^{80-363} showed similar PspC-binding activities. In contrast, Vn^{80-353} and further C-terminally truncated vitronectin fragments lacking the C-terminal heparin-binding domain (HBD3) did not bind to immobilized PspC-SH13 (Fig. 5*F*, supplemental Fig. S4*A*). In addition, binding of selected recombinant vitronectin fragments to *S. pneumoniae* D39Δ*cps* was analyzed by flow cytometry. The vitronectin fragments Vn^{80-396} and Vn^{80-363} bound to viable pneumococci and their binding was comparable to full length vitronectin. In contrast, vitronectin fragments lacking the C-terminal HBD3 (i.e. Vn^{80-353}, Vn^{80-339}, and Vn^{80-229}) bound to an extent of only 5-10% to the pneumococcal cell surface (Fig. 5*G*, supplemental Fig. S4*B*).

The sequence N-terminal to the HBD3 of immobilized vitronectin provides an additional structural binding site for PspC3—Pneumococci preferentially interact with host-cell bound vitronectin (4). Therefore, binding of FITC-labeled bacteria to immobilized vitronectin fragments was assayed. FITC-labeled D39Δ*cps* and PspC3-expressing recombinant *L. lactis* showed binding activity to Vn^{80-396}, Vn^{80-379}, Vn^{80-373}, Vn^{80-363}, as well as to Vn^{80-353} and Vn^{80-339}. A further C-terminal truncation, represented by the vitronectin fragment Vn^{80-229}, was necessary to substantially reduce the interaction of PspC-expressing pneumococci and lactococci with immobilized vitronectin (Fig. 6, *A* and *B*). In surface plasmon resonance measurements, PspC-SH13 showed similar binding activities to the immobilized vitronectin fragments Vn^{80-396} and Vn^{80-339}, but significantly reduced binding intensities to immobilized Vn^{80-229} (supplemental Fig. S5).

Vitronectin bound to PspC3 is functionally active and inhibits TCC deposition—Vitronectin controls the terminal complement pathway by binding the C5b-7 complex and thereby blocks the assembly and deposition of

the TCC (32, 33, 39). Vitronectin bound to PspC-SH13 inhibited TCC deposition in a dose-dependent manner. Vitronectin used at 50 µg/ml reduced TCC deposition by ~60% (Fig. 7). In contrast, the C3 convertase inhibitor Factor H showed no effect (Fig. 7). Thus, vitronectin, bound to PspC, maintains its central regulatory function and controls complement at the level of the terminal pathway.

DISCUSSION

Streptococcus pneumoniae utilize human multimeric vitronectin to adhere and invade host cells via the integrin route. Pneumococci exploit vitronectin as molecular bridge to access $\alpha_v\beta_3$-integrin receptors which results in an activation of the PI3K-Akt signaling pathway via the integrin-linked kinase, induces rearrangements of the host cell actin cytoskeleton and enhances pneumococcal internalization. The interaction between pneumococci and vitronectin is impaired after proteolytic treatment of the bacterial surface suggesting a proteinaceous nature of the vitronectin-binding factor (4). In this study, we showed that sortase- or lipid-anchored proteins are likely not involved in vitronectin-binding to the pneumococcal surface (Fig. 1*B*, supplemental Fig. S1*B*). However, removal of choline-binding proteins from the pneumococcal surface resulted in a significant decrease in vitronectin-binding (Fig. 1, *C* and *D*, supplemental Fig. S1*C*). PspC is a highly abundant choline-binding surface protein of pneumococci and *pspC*-deficient mutants showed a significantly reduced binding of vitronectin (Fig. 1*E*, supplemental Fig. S1*D*). In addition, pretreatment of pneumococcal strains expressing different PspC subtypes with anti-PspC antiserum diminished vitronectin-binding (Fig. 1*E*, supplemental Fig. S1*E-H*). These data suggest a role of PspC for the interaction of pneumococci with vitronectin. Classical PspC proteins consist of an N-terminal Factor H-binding region followed by either one or two α-helical SC-binding repeat domains (R1 and R2) connected by a flexible short random coil, a proline-rich region, and the choline-binding domain at the C-terminus. The PspC2 subtype present in *S. pneumoniae* ATCC33400 contains only one R domain, whereas PspC3 produced by *S. pneumoniae* D39 and TIGR4, respectively, comprises two R domains (21-23). Factor H did not compete with vitronectin for binding to PspC displayed on the pneumococcal surface or to immobilized purified PspC protein (Fig. 4*A*, supplemental Fig. S3*A*). In contrast, sIgA inhibited the interaction of vitronectin to pneumococcal surface-exposed PspC by approximately 70% as measured by flow cytometry (Fig. 4*B*, supplemental Fig. S3*B*). Binding of sIgA to immobilized recombinant PspC protein was also significantly inhibited by vitronectin, however, the efficiency was less pronounced under these conditions (Fig. 4*D*). SIgA has a high affinity (in the nanomolar range) to its hexapeptide binding motif in the mature PspC molecule (24, 25), whereas the affinity of vitronectin to its yet not finally defined binding epitope in PspC appears to be in the micromolar range, when calculating the dissociation constant using the 1:1 Langmuir binding model of the BIAevalution software (data not shown). In addition, these inhibition data suggest that sIgA and vitronectin do not recognize identical sequence motifs in the R domain(s), although the R domain(s) of PspC are essential for binding of both human proteins.

The PspC3 derivative PspC-SH13 bound efficiently vitronectin compared to PspC peptides comprising one R domain or only the Factor H-binding site (Fig. 2 and Fig. 3, supplemental Fig. S2). These results suggested that two interconnected R domains are essential for efficient vitronectin-binding. For ECM-recognizing adhesins of staphylococci and enterococci three distinct binding mechanisms are proposed, i.e. the ´tandem β-zipper´, the ´dock, lock, and latch´, and the ´collagen hug´ model. The two latter are characterized by two subdomains cooperating to capture the ligand molecule and a third subdomain securing the binding (44). These models, though, rely on the presence of Ig-like folds formed by antiparallel β-strands and hydrophobic interactions between adhesin and ligand. Recently, PavB of *S. pneumoniae* was shown to bind the adhesive glycoprotein fibronectin via its repetitive sequences (referred to as streptococcal surface repeats, SSUREs). Although one SSURE domain is sufficient for binding to fibronectin, the efficiency of the PavB-fibronectin interaction increases with the number of SSUREs (45). These data are in agreement with the assumption that the number of repeats influences protein structure, activity, and function (46). Biophysical and structural data

of PspC in complex with vitronectin are not available, which would provide comprehensive insights into the binding mechanism of the pneumococcal adhesin to the multifunctional human glycoprotein. PspC consists of charged "hot spots", which may serve as binding sites for vitronectin: (i) a highly charged region containing the SC-binding motif, and (ii) the R domain-connecting random coil with a high abundance of charged residues (21, 22). Charge plays a fundamental role in binding of vitronectin to PspC (Fig. 5A). Vitronectin contains three heparin-binding domains (HBDs) that are located to the residues 82–137, 175–219, and 348–361 (Fig. 5*E*) (39). The negatively charged glycosaminoglycans heparin, heparan sulfate and chondroitin sulfate A (Fig. 5*B-D*), but not the positively charged epsilon-aminocaproic acid and poly-L-lysine, inhibited PspC-binding to the C-terminal heparin-binding domain of vitronectin (data not shown). This suggests that the positively charged lysine residues within PspC are not involved in binding of vitronectin, whereas negatively charged (acidic) amino acid residues within PspC play a major role in this protein-protein interaction.

To localize the PspC-binding domain in vitronectin, recombinant vitronectin fragments were analyzed for their ability to bind PspC. Vitronectin fragments lacking the C-terminal heparin-binding domain did neither bind to immobilized PspC nor to the bacterial surface (Fig. 5, *F* and *G*, supplemental Fig. S4). These data indicate that PspC recognizes the C-terminal HBD, and thus resembles the binding features observed for proteins of other human pathogens, e.g. *H. influenzae* PE, *Moraxella catarrhalis* UspA2 and UspA2 variant proteins (UspA2V), and *Neisseria meningitidis* Opc (38, 39, 47). Further, PspC seems to interact with a region between HBD2 and HBD3 (residues 229-339) when vitronectin is immobilized on inert or biosensor surfaces (Fig. 6, *A* and *B*, supplemental Fig. S5). These differences in binding may be due to different conformations assumed by soluble *versus* host-cell bound vitronectin. Bacteria interacting with host ECM or serum proteins are often able to discriminate between particular states, i.e. soluble, immobilized, monomeric, or oligomeric structures, of a certain host protein. For example, PavA and PavB of *S. pneumoniae* preferentially recognize immobilized versus soluble fibronectin (14, 45). Similarly, the oral streptococci *S. mutans*, *S. sanguis* and *S. gordonii*, and viruses such as HIV adhere efficiently to a multimeric form of fibronectin that closely resembles *in vivo* matrix-associated fibronectin, but not to the soluble form (48-51).

Recruitment of human serum proteins to the bacterial surface allows complement control. Gram-negative pathogenic bacteria recruit plasma vitronectin to prevent the formation and deposition of the TCC and subsequent bacterial lysis. Recently, *H. influenzae* PE was shown to exclusively interact with the C-terminal heparin-binding domain of vitronectin to evade innate defense mechanisms (36-38). Encapsulated pneumococci are usually serum-resistant (52-54). However, the intimate contact of pneumococci with human host cells is associated with a loss of capsule polysaccharides, which renders these bacteria susceptible to innate immune responses (55-57). Therefore, we verified the inhibition of TCC deposition by vitronectin bound to PspC. Indeed, PspC-bound vitronectin inhibited the deposition of the TCC (Fig. 7) demonstrating that vitronectin is functionally active and may protect pneumococci against the attack of the complement system.

In conclusion, this study suggests that the multifunctional protein PspC plays a crucial role in binding the human adhesive glycoprotein vitronectin, besides being highly important for pneumococcal adhesion to host cells via the polymeric Ig receptor and interaction with proteins like secretory IgA and Factor H. Furthermore, the data indicate that two R domains within PspC, represented by PspC subtype 3, are required for the efficient interaction of *S. pneumoniae* with vitronectin. While PspC exclusively binds to the C-terminal heparin-binding domain of soluble vitronectin, it appears that a region directly N-terminal to the HBD3 of immobilized vitronectin, which mimics host cell-bound vitronectin *in vitro*, provides a further recognition site for PspC.

REFERENCES

1. Cartwright, K. (2002) Pneumococcal disease in western Europe: burden of disease, antibiotic resistance and management. *Eur J Pediatr* **161**, 188-195
2. Agarwal, V., Asmat, T. M., Luo, S., Jensch, I., Zipfel, P. F., and Hammerschmidt, S. (2010) Complement regulator Factor H mediates a two-step uptake of *Streptococcus pneumoniae* by human cells. *J Biol Chem* **285**, 23486-23495
3. Anderton, J. M., Rajam, G., Romero-Steiner, S., Summer, S., Kowalczyk, A. P., Carlone, G. M., Sampson, J. S., and Ades, E. W. (2007) E-cadherin is a receptor for the common protein pneumococcal surface adhesin A (PsaA) of *Streptococcus pneumoniae*. *Microb Pathog* **42**, 225-236
4. Bergmann, S., Lang, A., Rohde, M., Agarwal, V., Rennemeier, C., Grashoff, C., Preissner, K. T., and Hammerschmidt, S. (2009) Integrin-linked kinase is required for vitronectin-mediated internalization of *Streptococcus pneumoniae* by host cells. *J Cell Sci* **122**, 256-267
5. Romero-Steiner, S., Caba, J., Rajam, G., Langley, T., Floyd, A., Johnson, S. E., Sampson, J. S., Carlone, G. M., and Ades, E. (2006) Adherence of recombinant pneumococcal surface adhesin A (rPsaA)-coated particles to human nasopharyngeal epithelial cells for the evaluation of anti-PsaA functional antibodies. *Vaccine* **24**, 3224-3231
6. Rose, L., Shivshankar, P., Hinojosa, E., Rodriguez, A., Sanchez, C. J., and Orihuela, C. J. (2008) Antibodies against PsrP, a novel *Streptococcus pneumoniae* adhesin, block adhesion and protect mice against pneumococcal challenge. *J Infect Dis* **198**, 375-383
7. Shivshankar, P., Sanchez, C., Rose, L. F., and Orihuela, C. J. (2009) The *Streptococcus pneumoniae* adhesin PsrP binds to Keratin 10 on lung cells. *Mol Microbiol* **73**, 663-679
8. Voss, S., Gamez, G., and Hammerschmidt, S. (2012) Impact of pneumococcal microbial surface components recognizing adhesive matrix molecules on colonization. *Mol Oral Microbiol* **27**, 246-256
9. Attali, C., Frolet, C., Durmort, C., Offant, J., Vernet, T., and Di Guilmi, A. M. (2008) *Streptococcus pneumoniae* choline-binding protein E interaction with plasminogen/plasmin stimulates migration across the extracellular matrix. *Infect Immun* **76**, 466-476
10. Bergmann, S., Rohde, M., Chhatwal, G. S., and Hammerschmidt, S. (2001) alpha-Enolase of *Streptococcus pneumoniae* is a plasmin(ogen)-binding protein displayed on the bacterial cell surface. *Mol Microbiol* **40**, 1273-1287
11. Bergmann, S., Rohde, M., and Hammerschmidt, S. (2004) Glyceraldehyde-3-phosphate dehydrogenase of *Streptococcus pneumoniae* is a surface-displayed plasminogen-binding protein. *Infect Immun* **72**, 2416-2419
12. Hilleringmann, M., Giusti, F., Baudner, B. C., Masignani, V., Covacci, A., Rappuoli, R., Barocchi, M. A., and Ferlenghi, I. (2008) Pneumococcal pili are composed of protofilaments exposing adhesive clusters of Rrg A. *PLoS Pathog* **4**, e1000026
13. Papasergi, S., Garibaldi, M., Tuscano, G., Signorino, G., Ricci, S., Peppoloni, S., Pernice, I., Lo Passo, C., Teti, G., Felici, F., and Beninati, C. (2010) Plasminogen- and fibronectin-binding protein B is involved in the adherence of *Streptococcus pneumoniae* to human epithelial cells. *J Biol Chem* **285**, 7517-7524
14. Pracht, D., Elm, C., Gerber, J., Bergmann, S., Rohde, M., Seiler, M., Kim, K. S., Jenkinson, H. F., Nau, R., and Hammerschmidt, S. (2005) PavA of *Streptococcus pneumoniae* modulates adherence, invasion, and meningeal inflammation. *Infect Immun* **73**, 2680-2689
15. Rennemeier, C., Hammerschmidt, S., Niemann, S., Inamura, S., Zahringer, U., and Kehrel, B. E. (2007) Thrombospondin-1 promotes cellular adherence of gram-positive pathogens via recognition of peptidoglycan. *FASEB J* **21**, 3118-3132
16. Yamaguchi, M., Terao, Y., Mori, Y., Hamada, S., and Kawabata, S. (2008) PfbA, a novel plasmin- and fibronectin-binding protein of *Streptococcus pneumoniae*, contributes to fibronectin-dependent adhesion and antiphagocytosis. *J Biol Chem* **283**, 36272-36279
17. Gamez, G., and Hammerschmidt, S. (2012) Combat pneumococcal infections: adhesins as candidates for protein-based vaccine development. *Curr Drug Targets* **13**, 323-337
18. Bagnoli, F., Moschioni, M., Donati, C., Dimitrovska, V., Ferlenghi, I., Facciotti, C., Muzzi, A., Giusti, F., Emolo, C., Sinisi, A., Hilleringmann, M., Pansegrau, W., Censini, S., Rappuoli, R., Covacci, A., Masignani, V., and Barocchi, M. A. (2008) A second pilus type in

Streptococcus pneumoniae is prevalent in emerging serotypes and mediates adhesion to host cells. *J Bacteriol* **190**, 5480-5492
19. Barocchi, M. A., Ries, J., Zogaj, X., Hemsley, C., Albiger, B., Kanth, A., Dahlberg, S., Fernebro, J., Moschioni, M., Masignani, V., Hultenby, K., Taddei, A. R., Beiter, K., Wartha, F., von Euler, A., Covacci, A., Holden, D. W., Normark, S., Rappuoli, R., and Henriques-Normark, B. (2006) A pneumococcal pilus influences virulence and host inflammatory responses. *Proc Natl Acad Sci U S A* **103**, 2857-2862
20. Nelson, A. L., Ries, J., Bagnoli, F., Dahlberg, S., Falker, S., Rounioja, S., Tschop, J., Morfeldt, E., Ferlenghi, I., Hilleringmann, M., Holden, D. W., Rappuoli, R., Normark, S., Barocchi, M. A., and Henriques-Normark, B. (2007) RrgA is a pilus-associated adhesin in *Streptococcus pneumoniae*. *Mol Microbiol* **66**, 329-340
21. Brooks-Walter, A., Briles, D. E., and Hollingshead, S. K. (1999) The pspC gene of *Streptococcus pneumoniae* encodes a polymorphic protein, PspC, which elicits cross-reactive antibodies to PspA and provides immunity to pneumococcal bacteremia. *Infect Immun* **67**, 6533-6542
22. Iannelli, F., Oggioni, M. R., and Pozzi, G. (2002) Allelic variation in the highly polymorphic locus pspC of *Streptococcus pneumoniae*. *Gene* **284**, 63-71
23. Hammerschmidt, S., Talay, S. R., Brandtzaeg, P., and Chhatwal, G. S. (1997) SpsA, a novel pneumococcal surface protein with specific binding to secretory immunoglobulin A and secretory component. *Mol Microbiol* **25**, 1113-1124
24. Hammerschmidt, S., Tillig, M. P., Wolff, S., Vaerman, J. P., and Chhatwal, G. S. (2000) Species-specific binding of human secretory component to SpsA protein of *Streptococcus pneumoniae* via a hexapeptide motif. *Mol Microbiol* **36**, 726-736
25. Elm, C., Braathen, R., Bergmann, S., Frank, R., Vaerman, J. P., Kaetzel, C. S., Chhatwal, G. S., Johansen, F. E., and Hammerschmidt, S. (2004) Ectodomains 3 and 4 of human polymeric Immunoglobulin receptor (hpIgR) mediate invasion of *Streptococcus pneumoniae* into the epithelium. *J Biol Chem* **279**, 6296-6304
26. Zhang, J. R., Mostov, K. E., Lamm, M. E., Nanno, M., Shimida, S., Ohwaki, M., and Tuomanen, E. (2000) The polymeric immunoglobulin receptor translocates pneumococci across human nasopharyngeal epithelial cells. *Cell* **102**, 827-837
27. Orihuela, C. J., Mahdavi, J., Thornton, J., Mann, B., Wooldridge, K. G., Abouseada, N., Oldfield, N. J., Self, T., Ala'Aldeen, D. A., and Tuomanen, E. I. (2009) Laminin receptor initiates bacterial contact with the blood brain barrier in experimental meningitis models. *J Clin Invest* **119**, 1638-1646
28. Dave, S., Carmicle, S., Hammerschmidt, S., Pangburn, M. K., and McDaniel, L. S. (2004) Dual roles of PspC, a surface protein of *Streptococcus pneumoniae*, in binding human secretory IgA and factor H. *J Immunol* **173**, 471-477
29. Dieudonne-Vatran, A., Krentz, S., Blom, A. M., Meri, S., Henriques-Normark, B., Riesbeck, K., and Albiger, B. (2009) Clinical isolates of *Streptococcus pneumoniae* bind the complement inhibitor C4b-binding protein in a PspC allele-dependent fashion. *J Immunol* **182**, 7865-7877
30. Hammerschmidt, S., Agarwal, V., Kunert, A., Haelbich, S., Skerka, C., and Zipfel, P. F. (2007) The host immune regulator factor H interacts via two contact sites with the PspC protein of *Streptococcus pneumoniae* and mediates adhesion to host epithelial cells. *J Immunol* **178**, 5848-5858
31. Zipfel, P. F., Hallström, T., Hammerschmidt, S., and Skerka, C. (2008) The complement fitness factor H: role in human diseases and for immune escape of pathogens, like pneumococci. *Vaccine* **26 Suppl 8**, I67-74
32. Preissner, K. T. (1991) Structure and biological role of vitronectin. *Annu Rev Cell Biol* **7**, 275-310
33. Preissner, K. T., and Reuning, U. (2011) Vitronectin in vascular context: facets of a multitalented matricellular protein. *Semin Thromb Hemost* **37**, 408-424
34. Felding-Habermann, B., and Cheresh, D. A. (1993) Vitronectin and its receptors. *Curr Opin Cell Biol* **5**, 864-868

35. Chillakuri, C. R., Jones, C., and Mardon, H. J. (2010) Heparin binding domain in vitronectin is required for oligomerization and thus enhances integrin mediated cell adhesion and spreading. *FEBS Lett* **584**, 3287-3291
36. Hallström, T., Blom, A. M., Zipfel, P. F., and Riesbeck, K. (2009) Nontypeable *Haemophilus influenzae* protein E binds vitronectin and is important for serum resistance. *J Immunol* **183**, 2593-2601
37. Hallström, T., Singh, B., Resman, F., Blom, A. M., Morgelin, M., and Riesbeck, K. (2011) *Haemophilus influenzae* protein E binds to the extracellular matrix by concurrently interacting with laminin and vitronectin. *J Infect Dis* **204**, 1065-1074
38. Singh, B., Jalalvand, F., Morgelin, M., Zipfel, P., Blom, A. M., and Riesbeck, K. (2011) *Haemophilus influenzae* protein E recognizes the C-terminal domain of vitronectin and modulates the membrane attack complex. *Mol Microbiol* **81**, 80-98
39. Singh, B., Su, Y. C., and Riesbeck, K. (2010) Vitronectin in bacterial pathogenesis: a host protein used in complement escape and cellular invasion. *Mol Microbiol* **78**, 545-560
40. Hartel, T., Klein, M., Koedel, U., Rohde, M., Petruschka, L., and Hammerschmidt, S. (2011) Impact of glutamine transporters on pneumococcal fitness under infection-related conditions. *Infect Immun* **79**, 44-58
41. Asmat, T. M., Klingbeil, K., Jensch, I., Burchhardt, G., and Hammerschmidt, S. (2012) Heterologous expression of pneumococcal virulence factor PspC on the surface of *Lactococcus lactis* confers adhesive properties. *Microbiology* **158**, 771-780
42. Haupt, K., Reuter, M., van den Elsen, J., Burman, J., Halbich, S., Richter, J., Skerka, C., and Zipfel, P. F. (2008) The *Staphylococcus aureus* protein Sbi acts as a complement inhibitor and forms a tripartite complex with host complement Factor H and C3b. *PLoS Pathog* **4**, e1000250
43. Janulczyk, R., Iannelli, F., Sjoholm, A. G., Pozzi, G., and Bjorck, L. (2000) Hic, a novel surface protein of *Streptococcus pneumoniae* that interferes with complement function. *J Biol Chem* **275**, 37257-37263
44. Vengadesan, K., and Narayana, S. V. (2011) Structural biology of Gram-positive bacterial adhesins. *Protein Sci* **20**, 759-772
45. Jensch, I., Gamez, G., Rothe, M., Ebert, S., Fulde, M., Somplatzki, D., Bergmann, S., Petruschka, L., Rohde, M., Nau, R., and Hammerschmidt, S. (2010) PavB is a surface-exposed adhesin of *Streptococcus pneumoniae* contributing to nasopharyngeal colonization and airways infections. *Mol Microbiol* **77**, 22-43
46. Lin, I. H., Hsu, M. T., and Chang, C. H. (2012) Protein domain repetition is enriched in Streptococcal cell-surface proteins. *Genomics* **100**, 370-379
47. Hill, D. J., Whittles, C., and Virji, M. (2012) A Novel Group of *Moraxella catarrhalis* UspA Proteins Mediates Cellular Adhesion via CEACAMs and Vitronectin. *PLoS One* **7**, e45452
48. Chia, J. S., Yeh, C. Y., and Chen, J. Y. (2000) Identification of a fibronectin binding protein from *Streptococcus mutans*. *Infect Immun* **68**, 1864-1870
49. Lowrance, J. H., Hasty, D. L., and Simpson, W. A. (1988) Adherence of *Streptococcus sanguis* to conformationally specific determinants in fibronectin. *Infect Immun* **56**, 2279-2285
50. McNab, R., Holmes, A. R., Clarke, J. M., Tannock, G. W., and Jenkinson, H. F. (1996) Cell surface polypeptide CshA mediates binding of *Streptococcus gordonii* to other oral bacteria and to immobilized fibronectin. *Infect Immun* **64**, 4204-4210
51. Tellier, M. C., Greco, G., Klotman, M., Mosoian, A., Cara, A., Arap, W., Ruoslahti, E., Pasqualini, R., and Schnapp, L. M. (2000) Superfibronectin, a multimeric form of fibronectin, increases HIV infection of primary $CD4^+$ T lymphocytes. *J Immunol* **164**, 3236-3245
52. Hyams, C., Opel, S., Hanage, W., Yuste, J., Bax, K., Henriques-Normark, B., Spratt, B. G., and Brown, J. S. (2011) Effects of *Streptococcus pneumoniae* strain background on complement resistance. *PLoS One* **6**, e24581
53. Hyams, C., Yuste, J., Bax, K., Camberlein, E., Weiser, J. N., and Brown, J. S. (2010) *Streptococcus pneumoniae* resistance to complement-mediated immunity is dependent on the capsular serotype. *Infect Immun* **78**, 716-725
54. Yuste, J., Khandavilli, S., Ansari, N., Muttardi, K., Ismail, L., Hyams, C., Weiser, J., Mitchell, T., and Brown, J. S. (2010) The effects of PspC on complement-mediated immunity to *Streptococcus pneumoniae* vary with strain background and capsular serotype. *Infect Immun* **78**, 283-292

55. Hammerschmidt, S., Wolff, S., Hocke, A., Rosseau, S., Muller, E., and Rohde, M. (2005) Illustration of pneumococcal polysaccharide capsule during adherence and invasion of epithelial cells. *Infect Immun* **73**, 4653-4667
56. Weiser, J. N., and Kapoor, M. (1999) Effect of intrastrain variation in the amount of capsular polysaccharide on genetic transformation of *Streptococcus pneumoniae*: implications for virulence studies of encapsulated strains. *Infect Immun* **67**, 3690-3692
57. Weiser, J. N., Markiewicz, Z., Tuomanen, E. I., and Wani, J. H. (1996) Relationship between phase variation in colony morphology, intrastrain variation in cell wall physiology, and nasopharyngeal colonization by *Streptococcus pneumoniae*. *Infect Immun* **64**, 2240-2245
58. Petit, C. M., Brown, J. R., Ingraham, K., Bryant, A. P., and Holmes, D. J. (2001) Lipid modification of prelipoproteins is dispensable for growth in vitro but essential for virulence in *Streptococcus pneumoniae*. *FEMS Microbiol Lett* **200**, 229-233
59. Holmes, A. R., McNab, R., Millsap, K. W., Rohde, M., Hammerschmidt, S., Mawdsley, J. L., and Jenkinson, H. F. (2001) The pavA gene of *Streptococcus pneumoniae* encodes a fibronectin-binding protein that is essential for virulence. *Mol Microbiol* **41**, 1395-1408
60. Tettelin, H., Nelson, K. E., Paulsen, I. T., Eisen, J. A., Read, T. D., Peterson, S., Heidelberg, J., DeBoy, R. T., Haft, D. H., Dodson, R. J., Durkin, A. S., Gwinn, M., Kolonay, J. F., Nelson, W. C., Peterson, J. D., Umayam, L. A., White, O., Salzberg, S. L., Lewis, M. R., Radune, D., Holtzapple, E., Khouri, H., Wolf, A. M., Utterback, T. R., Hansen, C. L., McDonald, L. A., Feldblyum, T. V., Angiuoli, S., Dickinson, T., Hickey, E. K., Holt, I. E., Loftus, B. J., Yang, F., Smith, H. O., Venter, J. C., Dougherty, B. A., Morrison, D. A., Hollingshead, S. K., and Fraser, C. M. (2001) Complete genome sequence of a virulent isolate of *Streptococcus pneumoniae*. *Science* **293**, 498-506
61. Gasson, M. J. (1983) Plasmid complements of *Streptococcus lactis* NCDO 712 and other lactic streptococci after protoplast-induced curing. *J Bacteriol* **154**, 1-9
62. Ichihara, Y., and Kurosawa, Y. (1993) Construction of new T vectors for direct cloning of PCR products. *Gene* **130**, 153-154

FOOTNOTES

*This work was supported by Grants from the Deutsche Forschungsgemeinschaft DFG HA 3125/4-2 and the DFG-GRK840 (to S. H.).

$To whom correspondence should be addressed: Prof. Dr. Sven Hammerschmidt, Department Genetics of Microorganisms, Interfaculty Institute for Genetics and Functional Genomics, Ernst Moritz Arndt Universität Greifswald, Friedrich-Ludwig-Jahn-Strasse 15A, 17487 Greifswald, Germany, Phone: 0049-3834-864161, Fax: 0049-3834-864172, E-mail: sven.hammerschmidt@uni-greifswald.de

FIGURE LEGENDS

FIGURE 1. **Binding of human vitronectin to the pneumococcal surface is mediated by PspC.** Recruitment of soluble vitronectin to untreated or pretreated wild-type pneumococci or isogenic mutants (100 µl of 1 x 10^8 bacteria) was determined by flow cytometry. Bound vitronectin was detected using anti-human vitronectin antibodies, followed by an AlexaFluor488-conjugated anti-rabbit IgG. The results were expressed as GMFI x percentage of AlexaFluor488-labeled and gated bacteria. The mean values of at least three independent experiments are shown with error bars corresponding to SD. **, $p \leq 0.01$; ***, $p \leq 0.001$. Representative dot plots are shown in the supplemental Fig. S1.
A, Dose-dependent binding of soluble vitronectin to *S. pneumoniae* D39Δ*cps*.
B, Binding of soluble vitronectin to *S. pneumoniae* D39Δ*cps* (WT) and its isogenic mutants D39Δ*cps*Δ*lgt*, D39Δ*cps*Δ*lsp*, or D39Δ*cps*Δ*srtA*.
C-D, Binding of soluble vitronectin to pneumococci devoid of choline-binding proteins. *C*, *S. pneumoniae* D39Δ*cps* were incubated with vitronectin (2.5 µg/ml) in the absence (w/o) or presence of 5% choline chloride (ChoCl). *D*, Vitronectin bound to the pneumococcal surface in the absence (w/o) or presence of ChoCl is shown as dot plots of a representative flow cytometric analysis. The control dot plots show the GMFI x percentage of gated bacteria in the absence of vitronectin but after incubation with the antibodies.
E, Binding of soluble vitronectin to various pneumococcal strains, represented by low encapsulated (NCTC10319) or nonencapsulated (D39Δ*cps*, R800) pneumococci, and their isogenic Δ*pspC* mutants. The values for the vitronectin-binding to D39Δ*cps* were transferred from Figure 1B.
F, Inhibition of vitronectin-binding to pneumococci expressing different PspC subtypes with a mouse anti-PspC serum or mouse control serum. Vitronectin was used at a concentration of 1 µg/ml and 2.5 µg/ml, respectively.

FIGURE 2. **Vitronectin-binding to PspC subtype 3.**
A, Competitive inhibition of vitronectin-binding to pneumococci using a derivative of PspC subtype 3. *S. pneumoniae* D39Δ*cps* (100 µl of 1 x 10^8 bacteria) were incubated with vitronectin (1 µg/ml) and binding was competitively inhibited by the addition of increasing concentrations of PspC-SH13 (0-2 µM). Binding of vitronectin was determined by flow cytometry (for dot plots of a representative flow cytometric analysis, see supplemental Fig. S2) and data show the percentage of binding relative to vitronectin-binding to pneumococci in the absence of protein. The mean values of at least three independent experiments and the SD are shown. ***, $p \leq 0.001$.
B, Dose-dependent binding of soluble vitronectin to PspC-SH13. PspC-SH13, *S. aureus* Sbi, or *H. influenzae* PE were coated on microtiter plates (each 100 µl of 5 µg/ml) and incubated with increasing concentrations of vitronectin (0-25 µg/ml in 100 µl). Bound vitronectin was detected with anti-human vitronectin antibodies, followed by incubation with HRP-conjugated anti-goat antibodies. 1,2-phenylenediamine dihydrochloride was used as a substrate and the absorbance was measured at 492 nm. Results are the mean values ± SD of three independent experiments.
C, Surface plasmon resonance measurements of PspC-SH13 binding to immobilized vitronectin. Vitronectin was immobilized on a CM5 biosensor chip to a final rate of 350 response units (RU). PspC-SH13 was used as an analyte at a flow rate of 10 µl/min and the affinity surface was regenerated between subsequent sample injections with 12.5 mM sodium hydroxide. PspC-SH13 showed a dose-

dependent binding to vitronectin expressed in arbitrary response units. A control flow cell was used to subtract nonspecific signals.

FIGURE 3. **Vitronectin preferentially interacts with PspC proteins of subtype 3.**
A, Schematic model of the PspC subtypes 2 and 3 produced as N-terminally His_6-tagged protein derivatives in *E. coli*.
B, Schematic model of the PspC´-LPSTG-fusion proteins for the heterologous expression of PspC on the surface of *Lactococcus lactis*.
The Factor H-binding domain of PspC is shown in dark grey and the R domains (R1 and R2) of the different PspC variants are depicted in black. Each R domain contains the hexapeptide binding motif (Y/R)RNYPT for the secretory component (SC) of the pIgR and sIgA, respectively. LP, Leader peptide; CBD, choline-binding domain; P, proline-rich sequence; R, repeat domain.
C, Binding of vitronectin to immobilized PspC derivatives. PspC subtype 2 (PspC-SH2) or part structures of the mature PspC protein (PspC-SH3 or -SM2) were immobilized on microtiter plates (each 100 µl of 5 µg/ml) and incubated with increasing concentrations of vitronectin (0-25 µg/ml in 100 µl). PspC subtype 3 (PspC-SH13) is shown as the control and the value was transferred from Figure 2. Binding of vitronectin was detected as described in Figure 2. Results are the mean values ± SD of three independent experiments.
D, Binding of PspC derivatives to immobilized vitronectin measured by surface plasmon resonance. PspC-SH13 (representing subtype 3; 0.09 µM), PspC-SH2 (representing subtype 2; 1 µM), the mature N-terminal domain of PspC (PspC-SH3; 4 µM), and one R domain (PspC-SM2; 4 µM), respectively, were used as analytes at a flow rate of 10 µl/min and the affinity surface was regenerated between subsequent sample injections of proteins with 12.5 mM sodium hydroxide. The amount of PspC-binding to immobilized vitronectin is shown in arbitrary response units (RU).
E, Binding of PspC-expressing lactococci to immobilized vitronectin. PspC expression in *L. lactis* was induced and $2x10^8$ recombinant lactococci were labeled with FITC. Binding of FITC-labeled bacteria to immobilized vitronectin (50 µl of 10 µg/ml) was measured at 485 nm/538 nm (excitation/emission) and the number of bound bacteria was calculated. The mean values ± SD of at least three independent experiments performed in triplicates are shown. *, $p \leq 0.05$; **, $p \leq 0.01$; and ***, $p \leq 0.001$.

FIGURE 4. **Vitronectin and sIgA compete for binding to pneumococci and PspC.**
A, Factor H does not interfere with vitronectin-binding to viable pneumococci. *S. pneumoniae* D39Δ*cps* (100 µl of 1 x 10^8 bacteria) were incubated with 1 µg/ml biotinylated vitronectin (bioVn) in the presence of increasing concentrations of Factor H (0-20 µg/ml). Bound vitronectin was detected using Alexa488-conjugated streptavidin and binding was measured by flow cytometry. Binding of vitronectin in the absence of Factor H was defined as 100%. The mean values of at least three independent experiments and the SD are shown.
B, Secretory IgA inhibits vitronectin-binding to the pneumococcal surface. *S. pneumoniae* D39Δ*cps* (100 µl of 1 x 10^8 bacteria) were incubated with vitronectin (1 µg/ml) in the presence of sIgA (0-250 µg/ml). Binding of vitronectin was measured by flow cytometry as described in Figure 1, and vitronectin binding to pneumococci in the absence of sIgA was defined as 100%. The mean values ± SD of at least three independent experiments are shown. ***, $p \leq 0.001$.
A, and *B*, Representative dot plots are shown in supplemental Fig. S3.
C, Factor H does not compete with vitronectin for binding to immobilized PspC. In a total volume of 100 µl, Factor H (10 µg/ml) was incubated with increasing concentrations of vitronectin (0-40 µg/ml) and binding of vitronectin or Factor H to immobilized PspC subtype 3 (100 µl of 5 µg/ml) was measured. Results are shown as the mean values ± SD of at least three independent experiments.
D, Binding of sIgA to immobilized PspC is inhibited by vitronectin. In a total volume of 100 µl, increasing amounts of vitronectin (0-20 µg/ml) were employed to inhibit binding of secretory IgA (5 µg/ml) to immobilized PspC subtype 3 (100 µl of 5 µg/ml). Binding of vitronectin or sIgA was detected using specific antisera. The graph shows the mean values ± SD of at least three independent experiments. *, $p \leq 0.05$; **, $p \leq 0.01$.

FIGURE 5. **The C-terminal heparin-binding domain of vitronectin mediates binding to pneumococci and PspC.**
A, and *B*, Binding of vitronectin to PspC is charge-dependent and inhibited by heparin. PspC-SH13 was coated on microtiter plates (100 µl of 5 µg/ml) and binding of vitronectin (100 µl of 5 µg/ml) was measured in the presence of increasing concentrations of (A) NaCl (0-1 M) or (B) heparin (0-5000 µg/ml).
C, Schematic models of the recombinant vitronectin derivatives produced in HEK293T cells. The three heparin-binding domains are depicted in black.
D, Binding of soluble vitronectin to PspC requires the C-terminal HBD of vitronectin. Binding of soluble recombinant vitronectin peptides (each 100 µl of 5 µg/ml) to immobilized PspC-SH13, Sbi, or BSA (each 100 µl of 5 µg/ml) was determined by ELISA. The mean values ± SD of at least three independent experiments are shown in A, B, and D, respectively. **, $p \leq 0.01$; ***, $p \leq 0.001$.
E, The C-terminal HBD of vitronectin is essential for binding of soluble vitronectin to pneumococci. *S. pneumoniae* D39Δ*cps* (100 µl of 1 x 10^8 bacteria) were incubated with soluble vitronectin (1 µg/ml) or recombinant C-terminally truncated vitronectin fragments (each 5 µg/ml). Bound vitronectin was detected as described in Fig. 1 and measured by flow cytometry (for dot plots of a representative flow cytometric analysis, see supplemental Fig. S4). The results were expressed as GMFI multiplied with the percentage of fluorescent and gated bacteria. Results are shown as the mean values ± SD of at least three independent experiments. **, $p \leq 0.01$; ***, $p \leq 0.001$.

FIGURE 6. **Immobilization of vitronectin exposes an additional PspC-binding site in a region N-terminal to the HBD3.**
Binding of 2x10^8 FITC-labeled *S. pneumoniae* D39Δ*cps* (A) or recombinant *L. lactis* (B) to immobilized recombinant vitronectin peptides (each 50 µl of 5 µg/ml) was measured at 485 nm/ 538 nm (excitation/emission). BSA was used as a control protein. The number of bound bacteria was calculated and the graphs show the mean values ± SD of at least three independent experiments performed in duplicates. *, $p \leq 0.05$.

FIGURE 7. **Vitronectin bound to PspC3 is functionally active and inhibits TCC deposition.**
Vitronectin or Factor H was incubated at increasing concentrations (0-50 µg/ml in 100 µl) with immobilized PspC-SH12 (100µl of 5 µg/ml). After incubation with C5b-6 and C7, C8 and C9 were added to a total volume of 100 µl and TCC deposition was detected using anti-human C5b-9 monoclonal antibodies followed by HRP-conjugated anti-mouse IgG. Results are shown as the mean values ± SD of at least three independent experiments. **, $p \leq 0.01$; ***, $p \leq 0.001$.

TABLES

TABLE 1

Strains and plasmids used in this study

Strain or plasmid	Characteristics	Reference/source
Streptococcus pneumoniae		
P34	serotype 1	ATCC33400
P37	serotype 35A	NCTC10319
P137	R6Δ*lgt* (Δ*lgt*::Erm^r)	(58)
P173 (R800)	nonencapsulated derivative of R36A	(59)
P257 (D39)	serotype 2	NCTC7466
P261 (TIGR4)	serotype 4	(60)
PN107	TIGR4Δ*cps* (Δ*cps*::Km^r)	(30)
PN111	D39Δ*cps* (Δ*cps*::Km^r)	(15)
PN194	D39Δ*cps*Δ*pspC* (Δ*pspC*::Erm^r)	This study
PN220	D39Δ*cps*Δ*lgt* (Δ*lgt*::Erm^r)	This study
PN231	D39Δ*cps*Δ*lsp* (Δ*lsp*::Spc^r)	This study
PN299	D39Δ*cps*Δ*srtA* (Δ*srtA*::Erm^r)	This study
PN362	R800Δ*pspC* (Δ*pspC*::Spc^r)	This study
Lactococcus lactis		
Lacto 2	strain MG1363, plasmid free and prophage-cured derivative of NCDO 712	(61)
Lacto 22	Lacto 2 pPspC3	This study
Lacto 23	Lacto 2 pPspC2	This study
Escherichia coli		
DH5α	*Δ(lac)U169 endA1 gyrA46 hsdR17* Φ80Δ(lacZ)M15 *recA1 relA1 supE44 thi-1*	Novagen
Plasmids		
pGEM®-T easy	TA cloning vector for PCR products and blue-white colony selection, Amp^r	Promega
pBlue-Script II TKS(-)	TA cloning vector for PCR products and blue-white colony selection, Amp^r	(62)
pQSH22	pQE-30 with *pspC* gene region from *S. pneumoniae* ATCC33400, Amp^r	(23)
pQSV22spec	pQSH22 with *pspC* 5´and 3´flanking regions for mutagenesis, Amp^r, Spc^r	This study
p552	pGEM-T derivative with *spd_1243* 5´and 3´flanking regions for mutagenesis, Amp^r, Erm^r	This study
p556	pGEM-T derivative with *spd_0819* 5´and 3´flanking regions for mutagenesis, Amp^r, Spc^r	This study
p745	pBlue-Script derivative with *sp_1218* 5´and 3´flanking regions for mutagenesis, Amp^r, Erm^r	This study
pGKK1	pMSP3535 derivative expressing truncated *pspC3.4* from *S. pneumoniae* TIGR4 under P*nis*A promoter control, Erm^r	(41)
pPspC2	pMSP3535 derivative expressing *pspC2* from *S. pneumoniae* ATCC33400 under P*nis*A promoter control, Erm^r	This study
pPspC3	pMSP3535 derivative expressing *pspC3* from *S. pneumoniae* D39 under P*nis*A promoter control, Erm^r	This study

Amp, ampicillin; Km, kanamycin; Erm, erythromycin; Spc, spectinomycin; r, resistant

TABLE 2

Primers used in this study

Primer	Sequence[a]	Restriction site
SpcforClaI	5′-GCGCGCGCGCGCATCGATATCGATTTTCGTTCGTGAATAC-3′	*Cla*I
SpcrevClaI	5′-GCGCGCGCGCGCATCGATAATTAGAATGAAATATTTCCC-3′	*Cla*I
EryfwdAscI	5′-CGCGCGCGCGGGCGCGCCACGGTTCGTGTTCGTGCTG-3′	*Asc*I
EryrevAscI	5′-CGCGCGCGCGGGCGCGCCCGTAGGCGCTAGGGACCTC-3′	*Asc*I
lgt1fw	5’-GCCGTGCAGCTACCAGTCG-3’	none
lgt7rev	5’-CATCGATGACACGACCAAGC-3’	none
lsp1fwd	5’-CGGCCTTTTCAGAGCGCTATCC-3’	none
lsp4rev	5’-CCTTGAGTTCTTGGGCAAGTGC-3’	none
lsp2rev	5’-ATCGATCATGACTTCTACGAAGAGAGTC-3’	*Cla*I
lsp3fw	5’-ATCGATGTGGCAGATAGCTATC-3’	*Cla*I
SP_1218StartFor	5′-AAAGTAATGCGCCTGGATCA-3′	none
SP_1218StartRev	5′-AAAAGGCGCGCCCATTACTTGCTCGCGTTTCA-3′	*Asc*I
SP_1218EndFor	5′-AAAAGGCGCGCCCCTAACAGCTTTCAATCAACCA-3′	*Asc*I
SP_1218EndRev	5′-AAGTGACCAACTCGGCATTC-3′	none
N-PspC	5’-CGATGGATCCGTTTGCATCAAAAAGCGAAG-3’	*Bam*HI
PspCrev	5’- GCGCCCATGGTTTTTCTTTAACTTTATCTTCTTCTGCTGC-3’	*Nco*I

[a] restriction sites are underlined

FIGURES

FIGURE 1

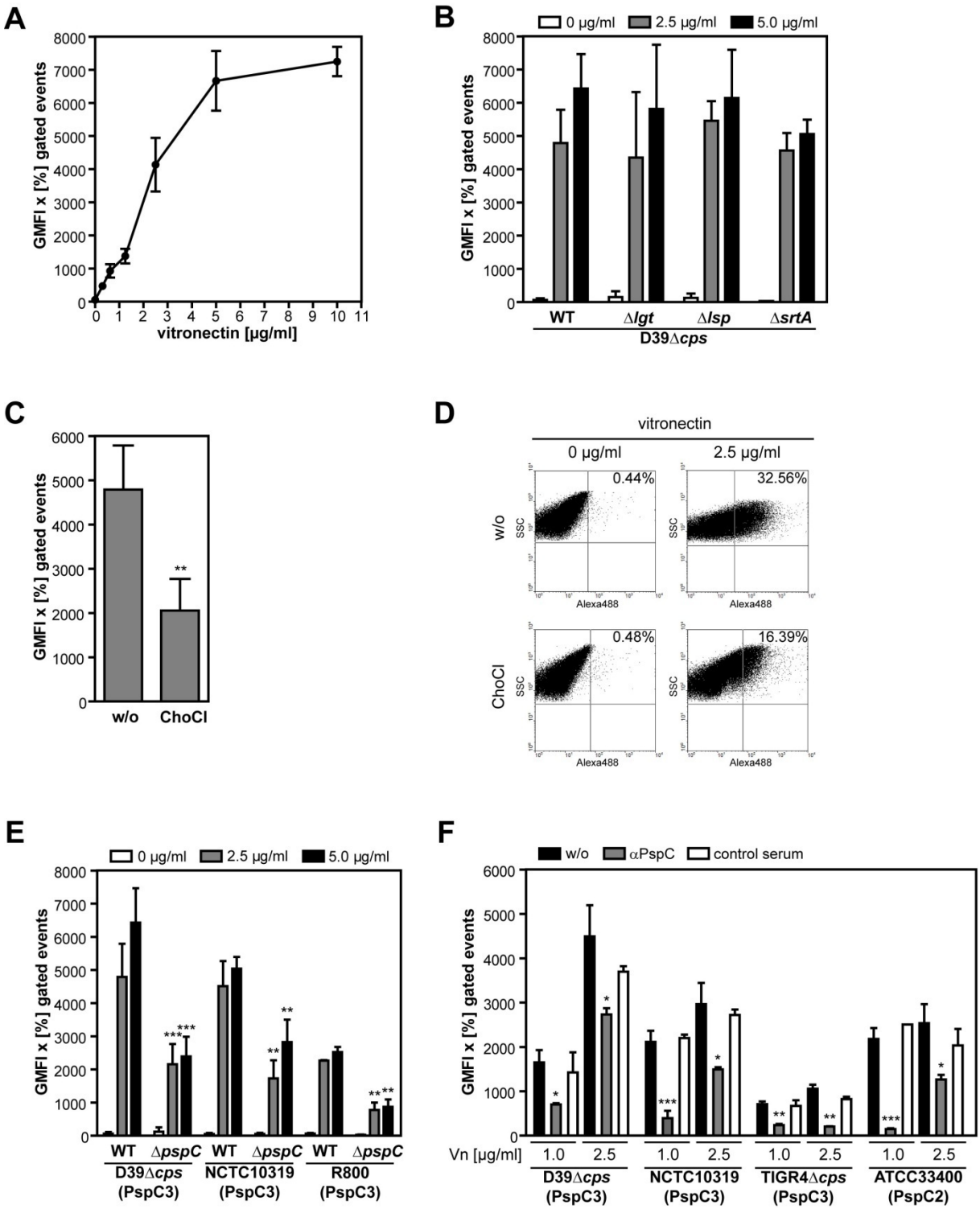

FIGURE 2

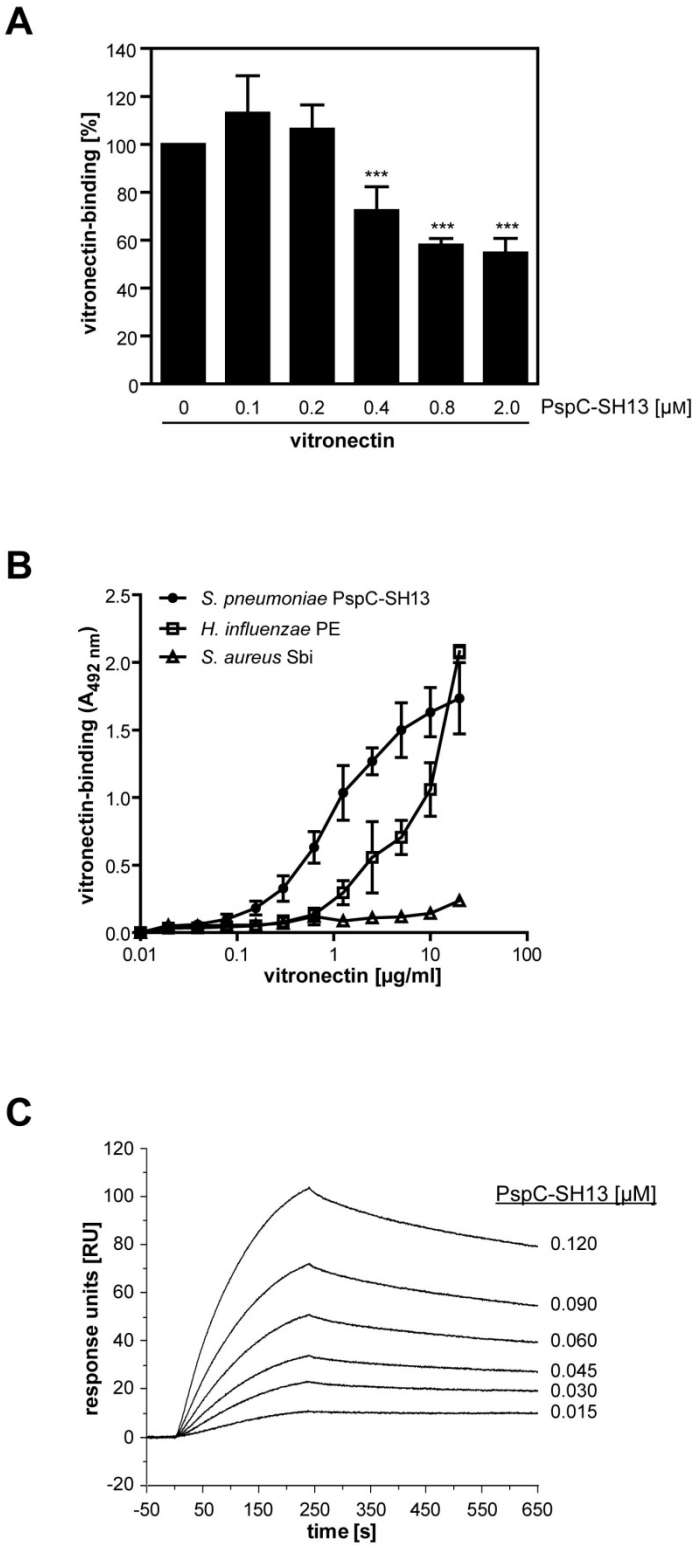
A
vitronectin-binding [%]
140
120
100
80
60
40
20
0
***
***
***
0
0.1
0.2
0.4
0.8
2.0
PspC-SH13 [µM]
vitronectin
B
S. pneumoniae PspC-SH13
H. influenzae PE
S. aureus Sbi
vitronectin-binding (A492 nm)
2.5
2.0
1.5
1.0
0.5
0.0
0.01
0.1
1
10
100
vitronectin [µg/ml]
C
response units [RU]
120
100
80
60
40
20
0
-20
-50
50
150
250
350
450
550
650
time [s]
PspC-SH13 [µM]
0.120
0.090
0.060
0.045
0.030
0.015

FIGURE 3

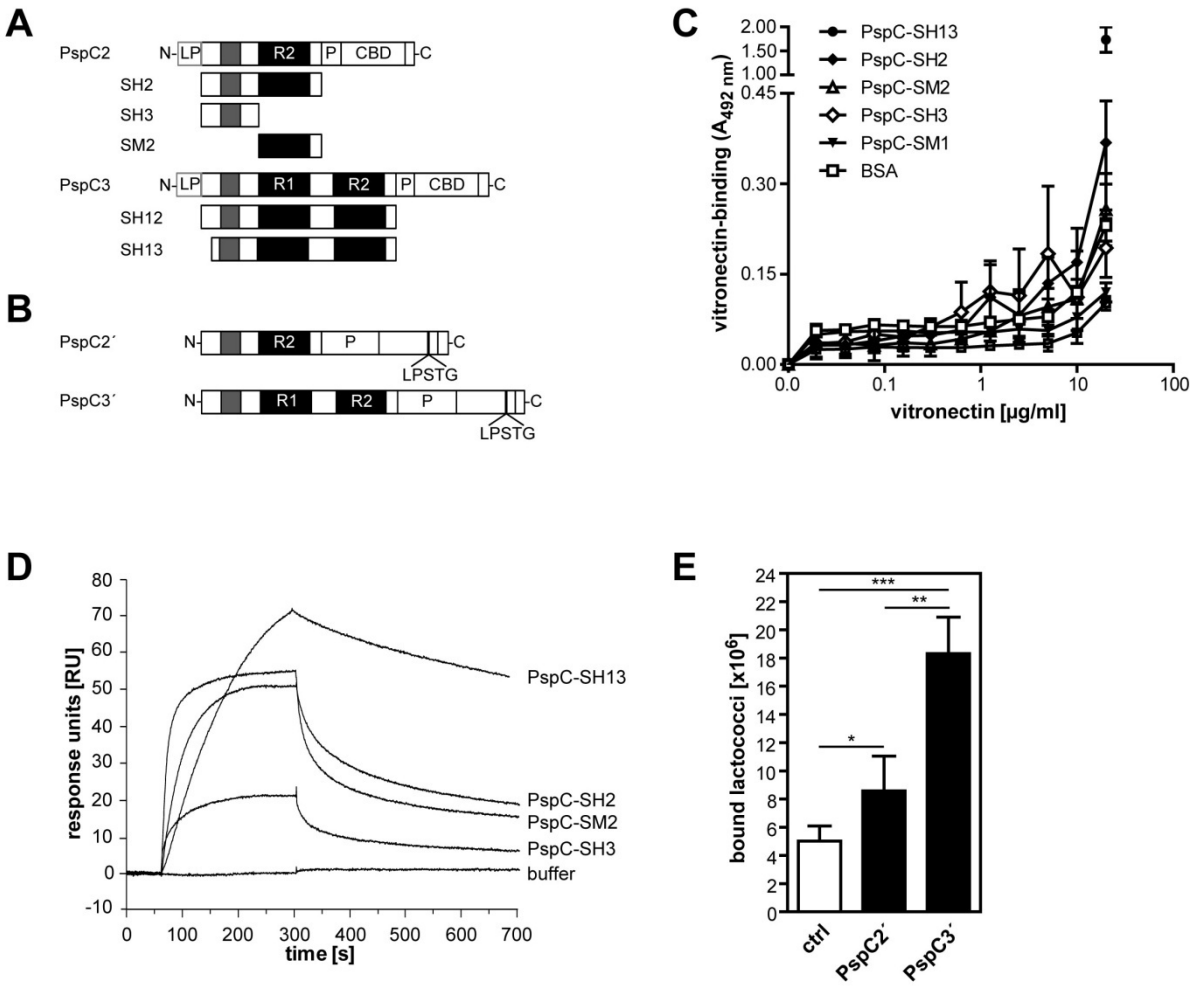
A
PspC2
N-LP
R2
P
CBD
C
SH2
SH3
SM2
PspC3
N-LP
R1
R2
P
CBD
C
SH12
SH13
B
PspC2´
N-
R2
P
C
LPSTG
PspC3´
N-
R1
R2
P
C
LPSTG
C
vitronectin-binding (A492 nm)
2.00
1.50
1.00
0.45
0.30
0.15
0.00
PspC-SH13
PspC-SH2
PspC-SM2
PspC-SH3
PspC-SM1
BSA
0.0
0.1
1
10
100
vitronectin [µg/ml]
D
response units [RU]
80
70
60
50
40
30
20
10
0
-10
0
100
200
300
400
500
600
700
time [s]
PspC-SH13
PspC-SH2
PspC-SM2
PspC-SH3
buffer
E
bound lactococci [x10^6]
24
22
20
18
16
14
12
10
8
6
4
2
0
***
**
*
ctrl
PspC2´
PspC3´

FIGURE 4

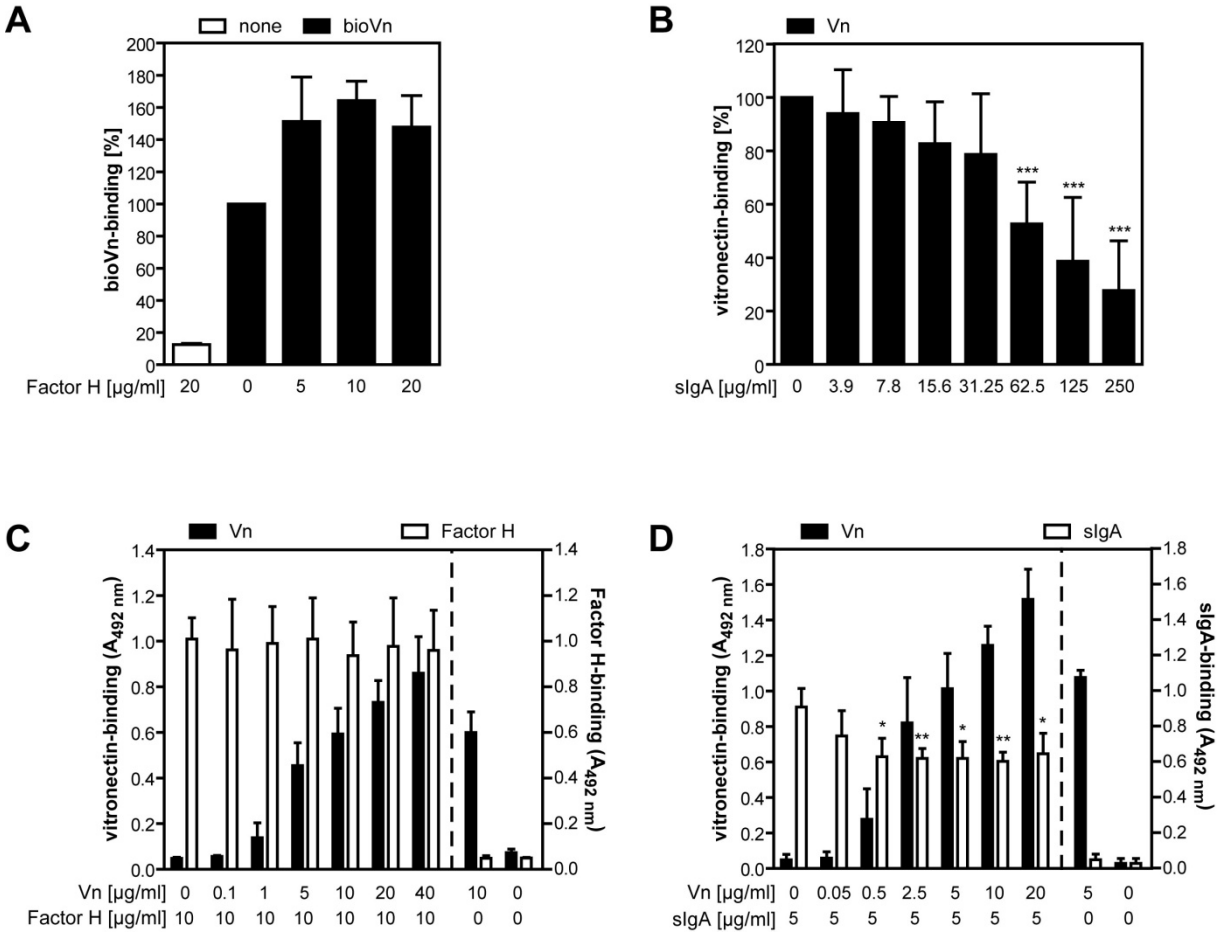
A
none
bioVn
bioVn-binding [%]
Factor H [µg/ml] 20 0 5 10 20
B
Vn
vitronectin-binding [%]
sIgA [µg/ml] 0 3.9 7.8 15.6 31.25 62.5 125 250
C
Vn
Factor H
vitronectin-binding (A492 nm)
Factor H-binding (A492 nm)
Vn [µg/ml] 0 0.1 1 5 10 20 40 10 0
Factor H [µg/ml] 10 10 10 10 10 10 10 0 0
D
Vn
sIgA
vitronectin-binding (A492 nm)
sIgA-binding (A492 nm)
Vn [µg/ml] 0 0.05 0.5 2.5 5 10 20 5 0
sIgA [µg/ml] 5 5 5 5 5 5 5 0 0

FIGURE 5

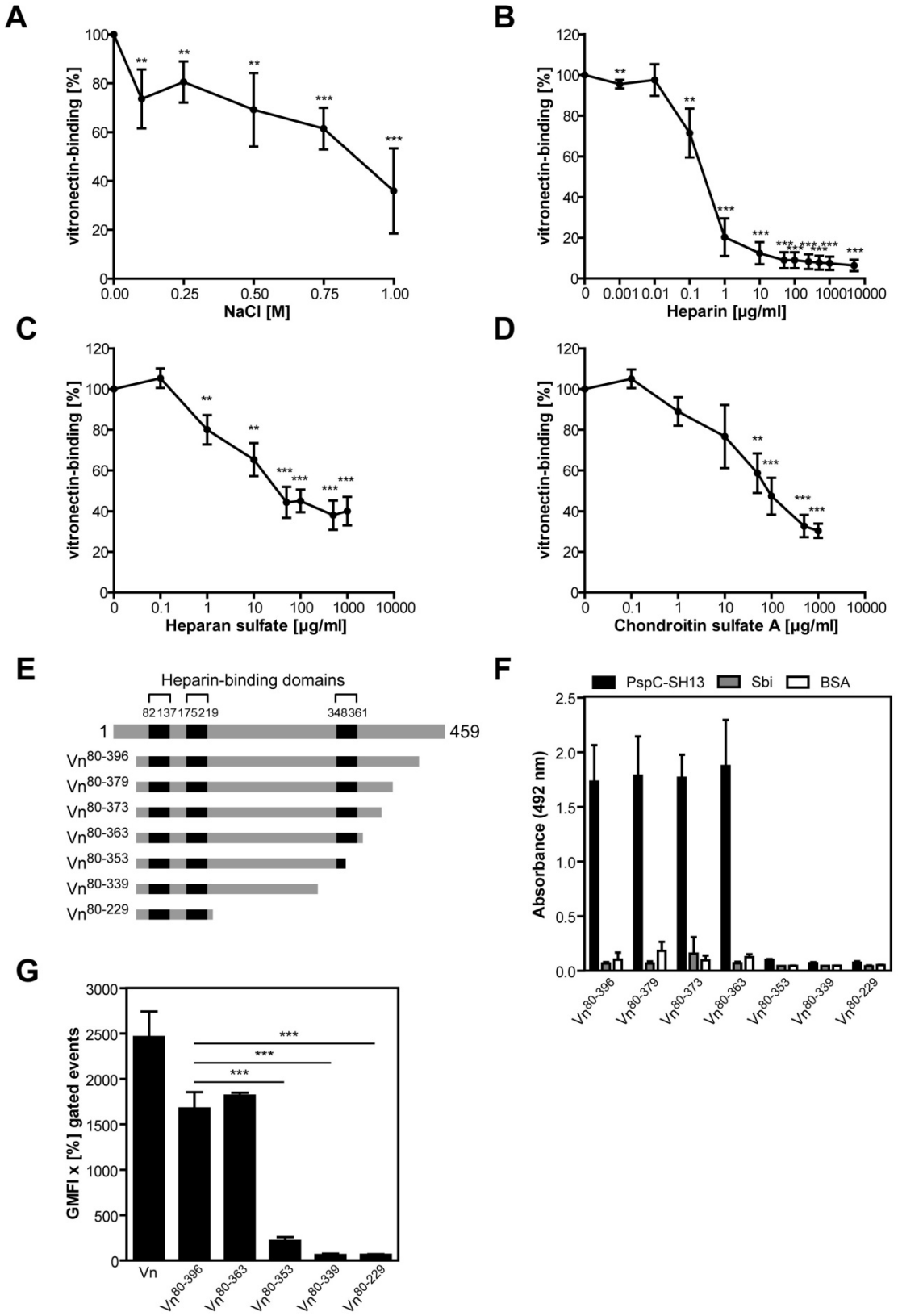
A
vitronectin-binding [%]
NaCl [M]
B
vitronectin-binding [%]
Heparin [µg/ml]
C
vitronectin-binding [%]
Heparan sulfate [µg/ml]
D
vitronectin-binding [%]
Chondroitin sulfate A [µg/ml]
E
Heparin-binding domains
82 137 175 219
348 361
1
459
Vn80-396
Vn80-379
Vn80-373
Vn80-363
Vn80-353
Vn80-339
Vn80-229
F
PspC-SH13
Sbi
BSA
Absorbance (492 nm)
G
GMFI x [%] gated events
Vn
Vn80-396
Vn80-363
Vn80-353
Vn80-339
Vn80-229

FIGURE 6

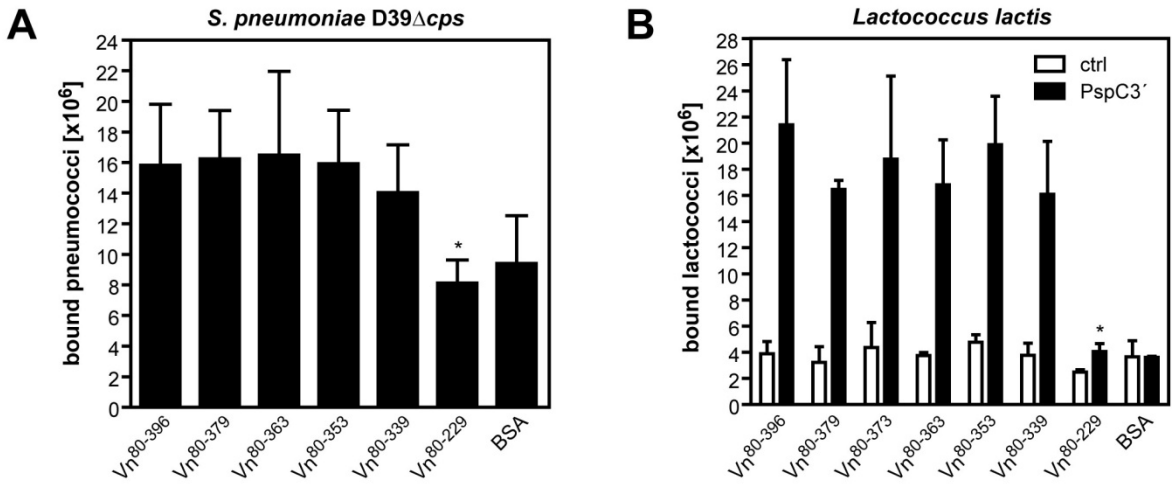
A
S. pneumoniae D39Δcps
bound pneumococci [x10^6]
0
2
4
6
8
10
12
14
16
18
20
22
24
*
Vn80-396
Vn80-379
Vn80-363
Vn80-353
Vn80-339
Vn80-229
BSA
B
Lactococcus lactis
bound lactococci [x10^6]
ctrl
PspC3´
0
2
4
6
8
10
12
14
16
18
20
22
24
26
28
*
Vn80-396
Vn80-379
Vn80-373
Vn80-363
Vn80-353
Vn80-339
Vn80-229
BSA

FIGURE 7

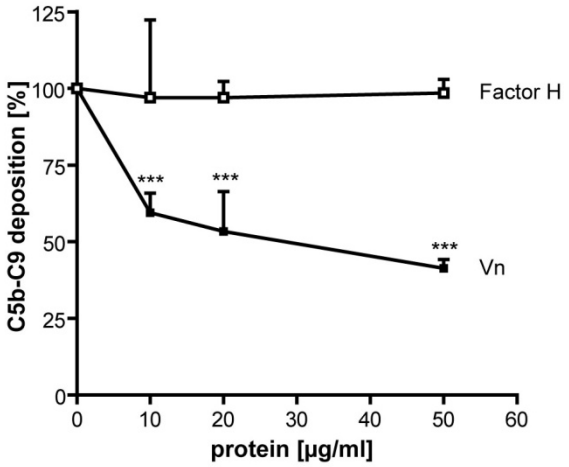
125
100
75
50
25
0
C5b-C9 deposition [%]
0
10
20
30
40
50
60
protein [µg/ml]
Factor H
Vn
***
***
***

SUPPLEMENTARY MATERIAL

FIGURE S1

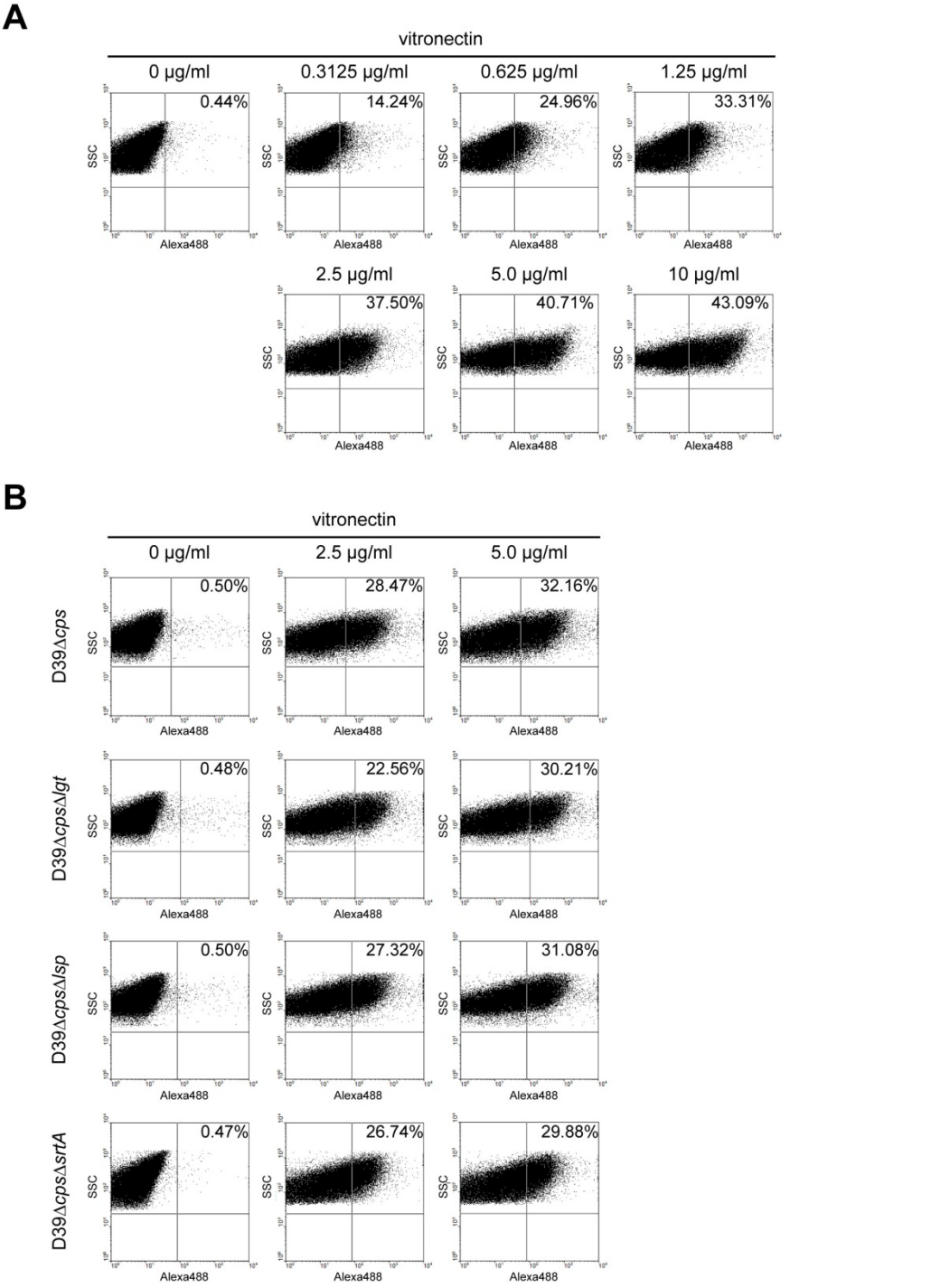

FIGURE S1

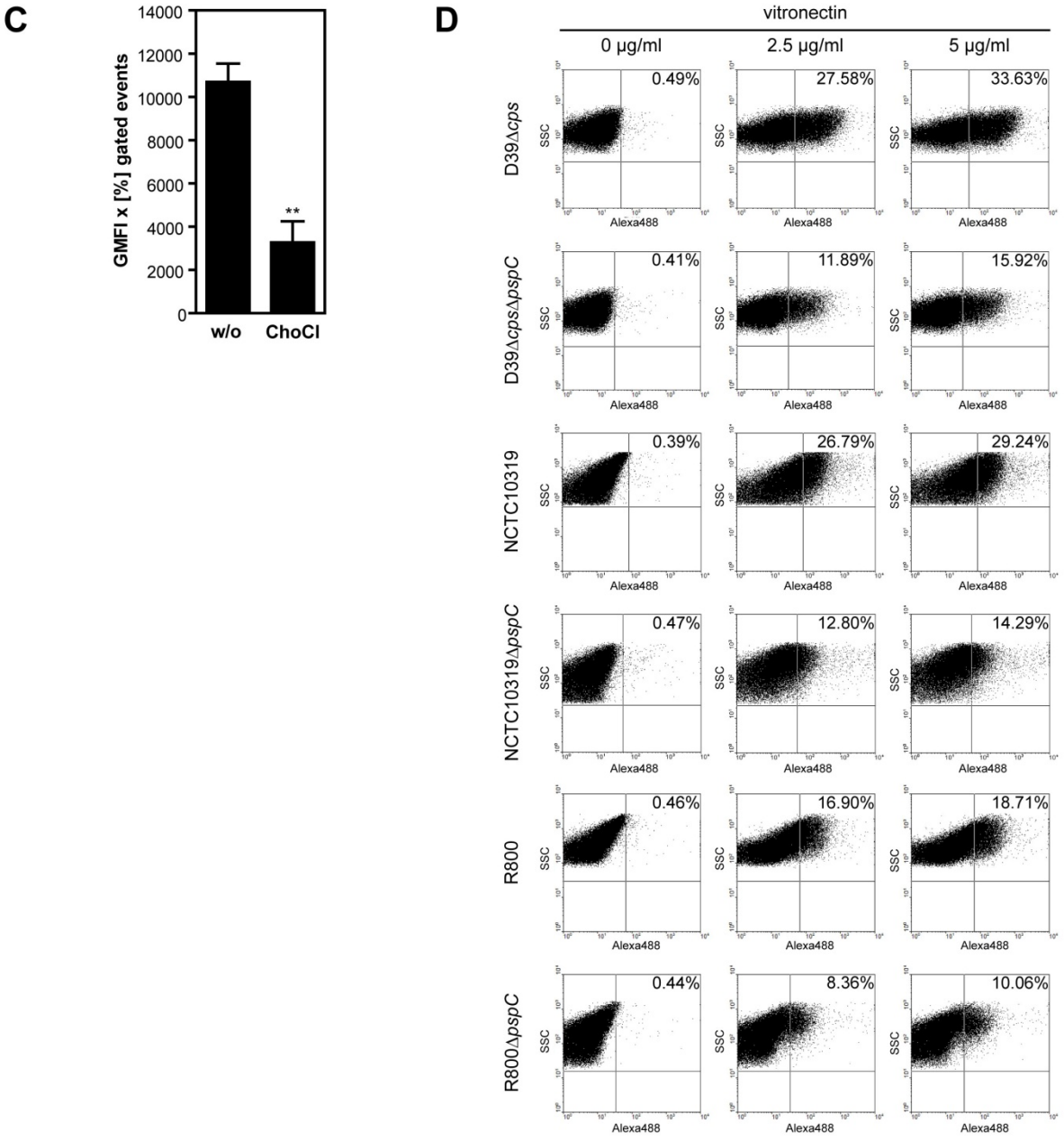
C
GMFI x [%] gated events
14000
12000
10000
8000
6000
4000
2000
0
**
w/o
ChoCl
D
vitronectin
0 µg/ml
2.5 µg/ml
5 µg/ml
D39Δcps
D39ΔcpsΔpspC
NCTC10319
NCTC10319ΔpspC
R800
R800ΔpspC
0.49%
27.58%
33.63%
0.41%
11.89%
15.92%
0.39%
26.79%
29.24%
0.47%
12.80%
14.29%
0.46%
16.90%
18.71%
0.44%
8.36%
10.06%
SSC
Alexa488

FIGURE S1

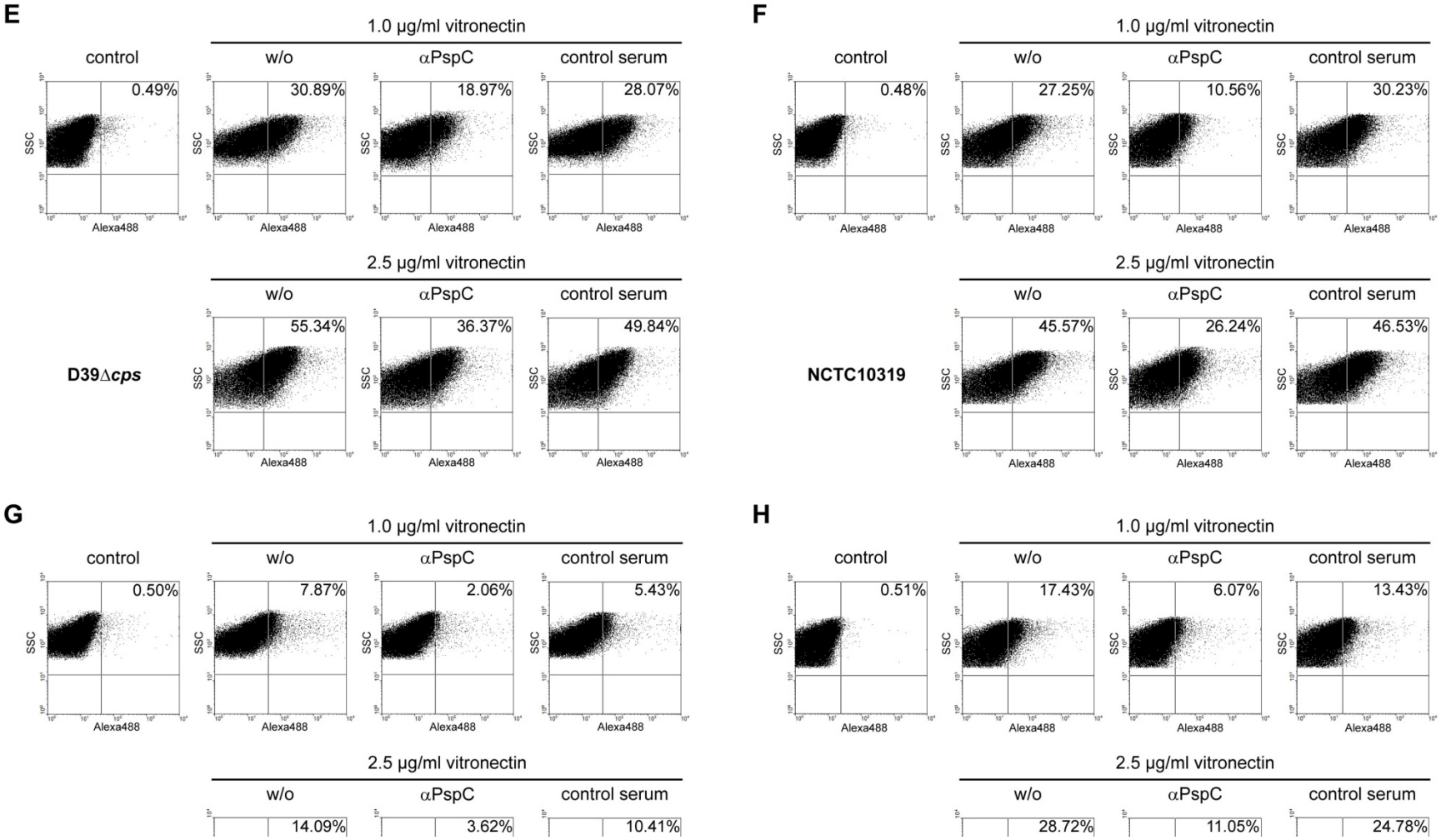
E
1.0 µg/ml vitronectin
control
w/o
αPspC
control serum
0.49%
30.89%
18.97%
28.07%
SSC
Alexa488
2.5 µg/ml vitronectin
w/o
αPspC
control serum
55.34%
36.37%
49.84%
D39Δcps
F
1.0 µg/ml vitronectin
control
w/o
αPspC
control serum
0.48%
27.25%
10.56%
30.23%
2.5 µg/ml vitronectin
w/o
αPspC
control serum
45.57%
26.24%
46.53%
NCTC10319
G
1.0 µg/ml vitronectin
control
w/o
αPspC
control serum
0.50%
7.87%
2.06%
5.43%
2.5 µg/ml vitronectin
w/o
αPspC
control serum
14.09%
3.62%
10.41%
H
1.0 µg/ml vitronectin
control
w/o
αPspC
control serum
0.51%
17.43%
6.07%
13.43%
2.5 µg/ml vitronectin
w/o
αPspC
control serum
28.72%
11.05%
24.78%

FIGURE S1. **PspC contributes to the recruitment of human vitronectin to the pneumococcal surface.**

A, *B*, *D-H*, Representative dot plots of flow cytometric analyses demonstrate the recruitment of soluble vitronectin to the surface of (A) *S. pneumoniae* D39Δ*cps*, (B) *S. pneumoniae* D39Δ*cps* and its isogenic mutants deficient in *lgt*, *lsp*, or *srtA*, (D) D39Δ*cps*, NCTC10319, R800 and their respective isogenic Δ*pspC* mutant, and (E-H) pneumococci pretreated with anti-PspC or control serum, (E) *S. pneumoniae* D39Δ*cps*, (F) NCTC10319, (G) TIGR4Δ*cps*, and (H) ATCC33400. Bound vitronectin was detected using rabbit anti-human vitronectin antibodies, followed by incubation with an AlexaFluor488-conjugated anti-rabbit IgG.

C, Flow cytometric analysis of PspC on the surface of pneumococci after treatment with choline chloride. *S. pneumoniae* D39Δ*cps* were incubated without (w/o) or with 5% choline chloride (ChoCl). The amount of surface-exposed PspC was detected using a mouse anti-SH12 serum, followed by incubation with a Cy5-conjugated anti-mouse IgG. The results were expressed as GMFI x percentage of Cy5-labeled and gated bacteria. The mean values of at least three independent experiments are shown with error bars corresponding to SD. **, $p \leq 0.01$.

FIGURE S2

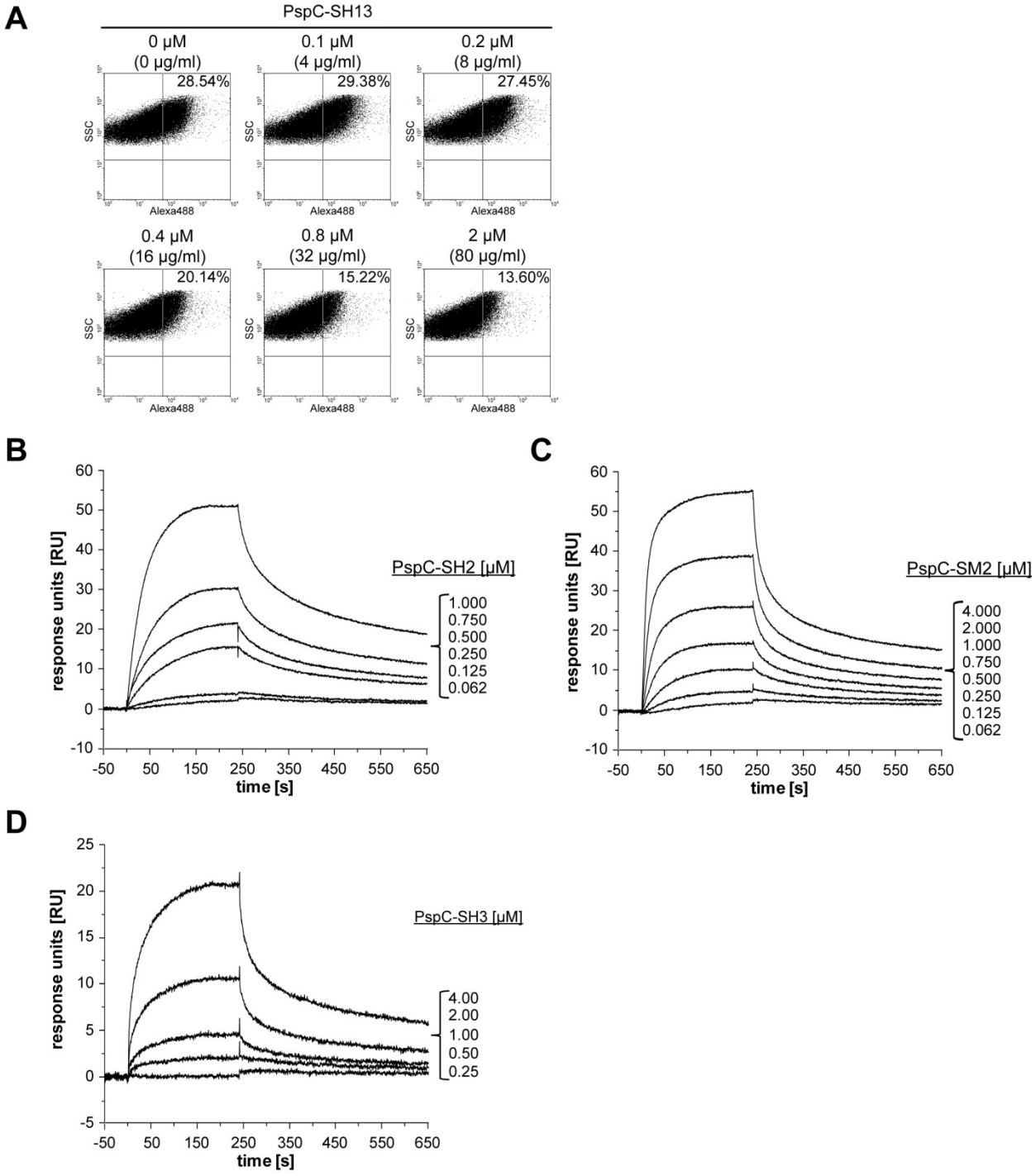

FIGURE S2. **Vitronectin-binding to PspC subtype 3.**
A, Competitive inhibition of vitronectin-binding to pneumococci using a derivative of PspC subtype 3 as analyzed by flow cytometry. Representative dot plots show the binding of vitronectin to *S. pneumoniae* D39Δ*cps* in the presence of increasing concentrations of PspC-SH13 (0-2 µM). Bound vitronectin was detected as described in Fig. S1.
B-D, Vitronectin was immobilized on a CM5 biosensor chip to a final rate of 350 response units (RU). PspC-SH2 (B), PspC-SM2 (C), and PspC-SH3 (D), respectively, were used in different concentrations as analytes in 0.05% Tween® 20/PBS (pH 7.4) at a flow rate of 10 µl/min and the affinity surface was regenerated between subsequent sample injections of proteins with 12.5 mM sodium hydroxide. Sensorgrams show the dose-dependent rates of PspC-binding to immobilized vitronectin expressed as arbitrary response units.

FIGURE S3

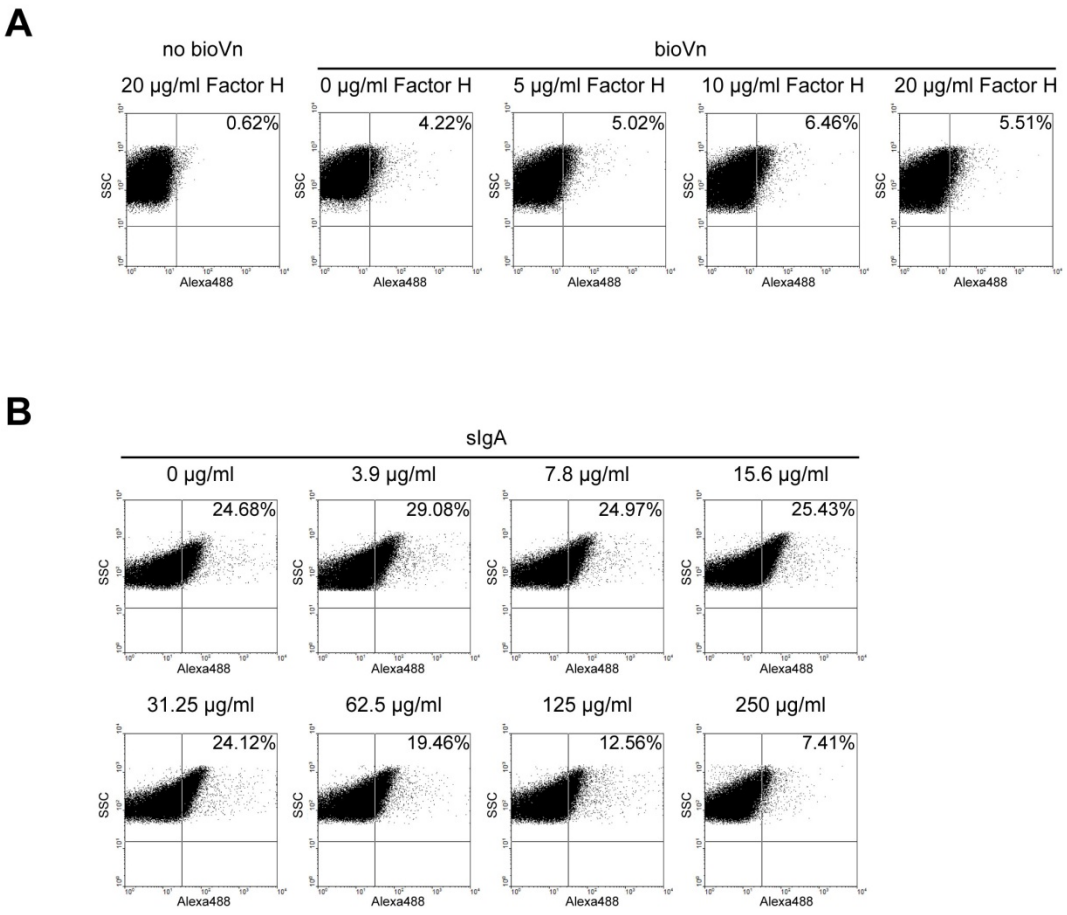

FIGURE S3. **Vitronectin and sIgA compete for binding to pneumococci and PspC.**
A, Vitronectin and Factor H do not compete for binding to pneumococci. *S. pneumoniae* D39Δ*cps* were incubated with 1 µg/ml biotinylated vitronectin (bioVn) in the presence of increasing concentrations of Factor H (0-20 µg/ml). Bound vitronectin was detected using Alexa488-conjugated streptavidin, analyzed by flow cytometry and vitronectin-binding is shown as dot plots of a representative experiment.
B, Competitive inhibition of vitronectin-binding to pneumococci by human secretory IgA (sIgA) as analyzed by flow cytometry. Representative dot plots illustrate the binding of vitronectin (1 µg/ml) to *S. pneumoniae* D39Δ*cps* (100 µl of 1 x 10^8 bacteria) in the presence of increasing concentrations of sIgA (0-250 µg/ml). Vitronectin bound to the pneumococcal surface was detected as described in Fig. S1.

FIGURE S4

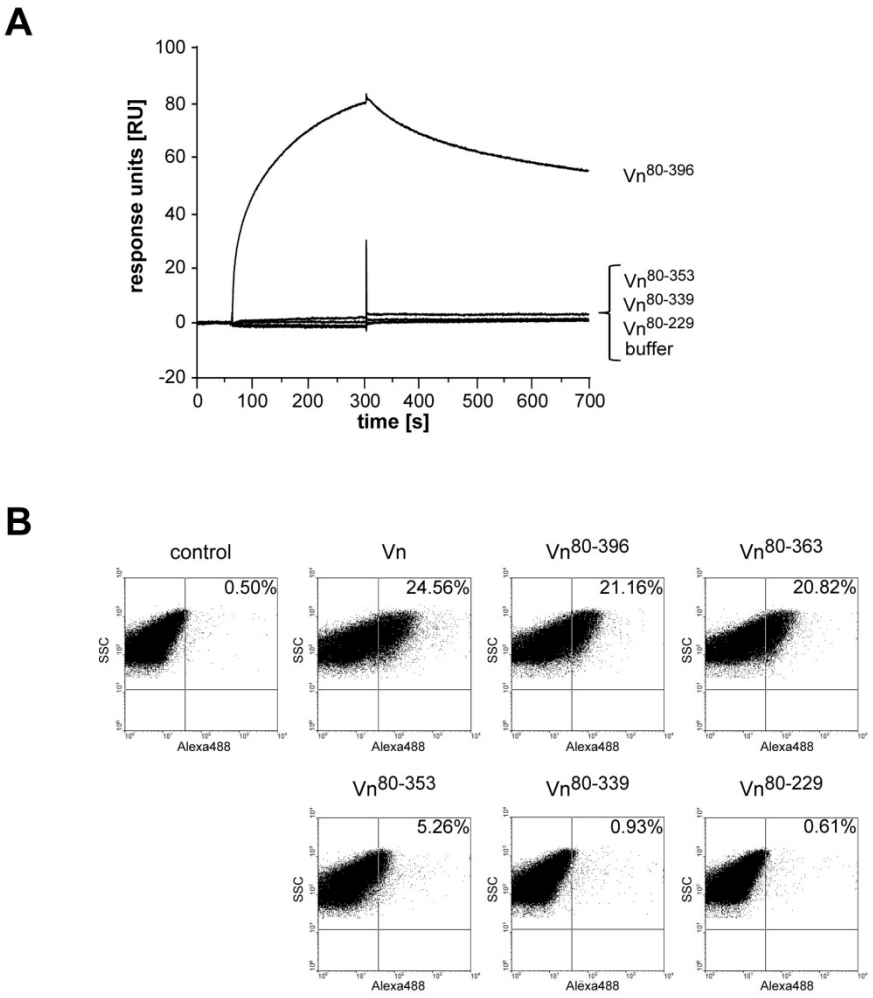

FIGURE S4. **The C-terminal heparin-binding domain of vitronectin is involved in binding to pneumococci and PspC.**
A, PspC-SH13 was immobilized on a CM5 biosensor chip to a final rate of 750 RU. The recombinant vitronectin fragments Vn^{80-396}, Vn^{80-339}, and Vn^{80-229}, respectively, were used as analytes in HNET buffer at a concentration of 50 µg/ml at a flow rate of 10 µl/min. The affinity surface was regenerated between subsequent sample injections of proteins with 2 M NaCl. In contrast to Vn^{80-396}, binding of vitronectin fragments that lack the entire C-terminal heparin-binding domain (i.e. Vn^{80-353}, Vn^{80-339}, and Vn^{80-229}) to immobilized PspC-SH13 was completely absent.
B, Representative dot plots show the binding of soluble vitronectin (1 µg/ml) or recombinant human vitronectin fragments (each 5 µg/ml) to *S. pneumoniae* D39Δ*cps* as analyzed by flow cytometry.

FIGURE S5

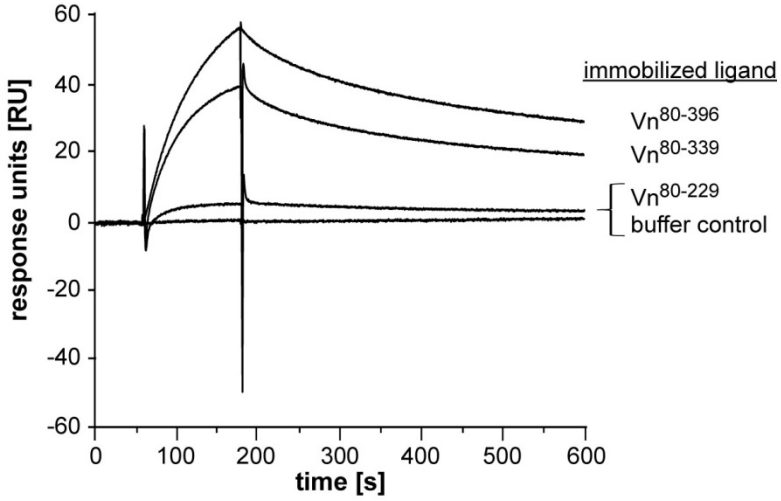

FIGURE S5. **Immobilization of vitronectin exposes an additional PspC-binding site in a region N-terminal to the HBD3.**
The recombinant vitronectin fragments Vn^{80-396}, Vn^{80-339}, and Vn^{80-229}, respectively, were immobilized on a CM5 biosensor chip to a final rate of 3400 RU, 1900 RU, and 1600 RU, respectively. PspC-SH13 was used as an analyte in 0.05% Tween® 20/PBS (pH 7.4) at a concentration of 0.05 µM at a flow rate of 10 µl/min. Sodium hydroxide (50 mM) was used to remove bound protein from the affinity surface. The sensorgram shows that PspC-SH13 binds to the immobilized vitronectin fragments Vn^{80-396} and Vn^{80-339}, and to a lower extent to Vn^{80-229}.